Methane distribution and oxidation around the Lena Delta in summer 2013

Ingeborg Bussmann, Steffen Hackbusch, Patrick Schaal, Antje Wichels

Alfred Wegener Institute for Polar and Marine Research, Marine Station Helgoland, Kupromenade 201, 27498 Helgoland, Germany

Correspondence to: Ingeborg Bussmann (Ingeborg.bussmann@awi.de)

Abstract. The Lena River is one of the largest Russian rivers draining into the Laptev Sea. The predicted increases in global temperatures are expected to cause the permafrost areas surrounding the Lena Delta to melt at increasing rates. This melting will result in high amounts of methane reaching the waters of the Lena and the adjacent Laptev Sea. The only biological sink for reducing methane concentrations within this system is methane oxidation by methanotrophic bacteria. However, the polar estuary of the Lena River, due to its strong fluctuations in salinity and temperature, is a challenging environment for bacteria. We determined the activity and abundance of aerobic methanotrophic bacteria by a tracer method and the quantitative polymerase chain reaction. We described the methanotrophic population with a molecular finger printing method (monooxygenase intergenic spacer analysis), as well as the methane distribution (via a head-space method) and other abiotic parameters in the Lena Delta in September 2013.

"Riverine water" (S <5) contained a median methane concentration of 22 nmol L^{-1}, "mixed water" (5 < S < 20) contained a median of 19 nmol L^{-1} and "polar water" (S > 20) contained a median of 28 nmol L^{-1}. The Lena River was not the methane source for surface water, and the bottom water methane concentrations were mainly influenced by the concentration in surface sediments. However, the methane oxidation rate in riverine and polar water was very similar (0.419 and 0.400 nmol $L^{-1} d^{-1}$), but with a higher relative abundance of methanotrophs and a higher "estimated diversity" in the "riverine water" than in the "polar water". The turnover times of methane ranged from 167 d in "mixed water" and 91 d in "riverine water" to only 36 d in "polar water". The environmental parameters influencing the methane oxidation rate and the methanotrophic population also differed between the water masses. Thus, we postulate a riverine methanotrophic population limited by sub-optimal temperatures and substrate concentrations and a polar methanotrophic population that is well adapted to the cold and methane poor environment, but limited by the nitrogen content. The diffusive methane flux into the atmosphere ranged from 4 to 163 μmol m^2 d^{-1} (median 24). For the total methane inventory of the investigated area, the diffusive methane flux was responsible for 8% loss, compared to only 1% of the methane consumed by the methanotrophic bacteria within the system. Our results underscore the importance of measuring the methane oxidation activities in polar estuaries, and they indicate a population-level adaptation of the water column methanotrophs to riverine versus polar conditions.

1 Introduction

Methane is an important greenhouse gas and concerted efforts are ongoing to assess its different sinks and sources. Overall, about two-thirds of the emissions are caused by human activities; the remaining third is from natural sources (Kirschke et al., 2013). Methane sources and sinks also vary with latitude (Saunois et al., 2016). For example, at polar latitudes, methane sources include wetlands, natural gas wells and pipelines, thawing permafrost, and methane hydrate associated with decaying offshore permafrost (Nisbet et al., 2014). More data are needed to resolve the divergence between top-down and bottom-up estimates of methane sources, but the measurement network that focuses on methane concentrations and isotopes is rather sparse (Nisbet et al., 2014). Better measurements, both spatial and temporal, are essential for identifying and quantifying methane sources.

One poorly studied area is the Arctic Ocean, the intercontinental sea that is surrounded by the landmasses of Alaska/U.S.A., Canada, Greenland, Norway, Iceland and Siberia/Russia. This ocean represents about 1% of the global ocean volume but receives about 10% of all global runoff (Lammers et al., 2001). It has a central deep basin and is characterised by extensive shallow shelf areas, including the Barents Sea, Kara Sea, Laptev Sea, East Siberian Sea, Chukchi Sea and Beaufort Sea. Methane sources in these arctic areas can include the thawing methane hydrates off Svalbard (Westbrook et al., 2009), and ebullition of methane from diverse geologic sources (Mau et al., 2017;Shakhova et al., 2014). In addition, the extensive shallow-water areas of the Arctic continental shelf are underlain by permafrost, which was formed under terrestrial conditions and subsequently submerged by post-glacial rises in sea level. Methane can be trapped within this permafrost, as well as below its base (Rachold et al., 2007).

The fate of the released methane depends on several factors. When methane leaves the sediment (either by diffusion or by ebullition) at water depths > 200 m, most of it will be dissolved into the water below the thermocline and will not reach surface waters or the atmosphere (Gentz et al., 2013;Myhre et al., 2016). However, ebullition at shallow water depths represents a shortcut, as most of this methane will not dissolve into the water and instead will reach the atmosphere. For lakes, ebullition is estimated to contribute 18 to 22% of the total emission (Del Sontro et al. 2016). Methane that does dissolve in the water can be oxidised by methane oxidising bacteria (MOB). These microorganisms can convert methane to CO_2 and water, and therefore can have an important effect on reducing the greenhouse effect considerably (Murrell and Jetten, 2009). Water column methane oxidation (MOX) is therefore the final sink for methane before it is released to the atmosphere. The amount of methane consumed by this microbial filter depends on the abundance of these microorganisms and the water current patterns (Steinle et al., 2015), but the efficiency of MOBs is determined mostly by methane concentrations and temperature (Lofton et al., 2014). Nevertheless, not much is known about the abundance and population structure of marine, polar MOBs.

The area of the Laptev and East Siberian Sea has been a scientific focus of polar methane studies. The partial thawing of the permafrost on the shallow East Siberian Arctic Shelf is considered to be responsible for the very high dissolved methane concentrations in the water column (> 500 nmol L^{-1}) and elevated methane concentrations in the atmosphere (Shakhova et al., 2014). Other authors have shown that, in the Laptev Sea, methane released from thawing permafrost is efficiently oxidised by microorganisms in the overlying unfrozen sediments, so that methane concentrations in the water column were close to normal background levels (Overduin et al., 2015). High-resolution, simultaneous measurements of methane in the atmosphere and above

the surface waters of the Laptev and East Siberian Seas have revealed that the sea-air methane flux is dominated by diffusive fluxes, not bubble fluxes (Thornton et al., 2016).

The aim of the present study was to obtain an overview of the methane distribution in the northern parts of the Lena Delta and to gain the first key insights into the role of methane-oxidising bacteria (MOB) in the methane cycle occurring in this area. An additional aim was to assess which environmental factors determine the methane distribution and its oxidation in this delta.

2 Material and Methods

2.1 Study site

The Lena Expedition was conducted in late summer, 1–7 September, 2013, on board the Russian R/V "Dalnie Zelentsy" of the Murmansk Marine Biological Institute, in the areas surrounding the Lena River Delta region, Laptev Sea, Siberia. Four transects around the Lena Delta were investigated (Figure 1). Transect 1 started near the Bykovski peninsula and headed towards the northeast. This transect was the same as in 2010 (Bussmann, 2013b). Transect 4 was located near the mouth of the Trofimovskaya Channel and Transect 6 was located at the northern point of the Delta.

Hydrography (temperature, salinity, currents) and water chemistry [dissolved organic carbon (DOC), pH, oxygen, total dissolved nitrogen (TDN)] were determined as described previously (Gonçalves-Araujo et al., 2015;Dubinenkov et al., 2015). Water samples were taken using Niskin bottles at the surface and at discrete depths chosen based on salinity profiles. Samples for methane analyses were taken from surface and bottom waters, and at the pycnoclines at the deeper stations. The sediment surface was sampled with a grab sampler.

We classified the water masses as follows "riverine water" with a salinity (S) < 5, "mixed water" with 5 < S < 20 and "polar water" with S > 20, as modified from (Caspers, 1959).

2.2 Water sampling and gas analysis

Duplicate serum bottles (120 ml) were filled from the water sampler using thin silicon tubing. The bottles were flushed extensively with sample water (to ensure no contact with the atmosphere) and finally closed with butyl rubber stoppers; excess water could escape via a needle in the stopper. Samples were poisoned with 0.3 ml of 25% H_2SO_4, stored upside down at temperatures < 15°C, and analysed after 4 months. Glass bottles and butyl stoppers are relatively methane tight and acidification of water samples results in good long-term sample preservation (Magen et al., 2014;Taipale and Sonninen, 2009). However, we cannot exclude the possibility that some methane was lost from the samples. In the home laboratory, 20 ml of nitrogen was added to extract the methane from the water phase, and excess water was allowed to escape via a needle. The samples were vigorously shaken and equilibrated for at least two hours. The volumes of the water and gas phases were calculated by differential weighing.

For sediment samples, 3 ml of surface sediment was transferred into 12 ml glass ampoules using cut off syringes. The samples were poisoned with 2 ml NaOH (1 mol L^{-1}) and sealed with butyl rubber stoppers.

Headspace methane concentrations were analysed in the home laboratory with a gas chromatograph (GC 2014, Shimadzu) equipped with a flame ionisation detector and a molecular sieve column (Hay Sep N, 80/100, Alltech). The temperatures of the oven, the injector and detector were 40, 120 and 160 °C, respectively. The carrier gas (N_2) flow was 20 ml min^{-1}, with 40 ml min^{-1} H_2 and 400 ml min^{-1} synthetic air. Gas standards (Air Liquide) with methane concentrations of 10 and 100 ppm were used for calibration. The calculation of the methane concentration was performed according to (Magen et al., 2014), taking into account the different methane solubilities at the wide range of salinities (1–33). The precision of the calibration line was $r^2 = 0.99$ and the reproducibility of the samples was 7%. The methane-related data set is available at www.pangaea.de, doi:10.1594/PANGAEA.868494, 2016.

2.3 Determination of the methane oxidation rate (MOX)

The MOX was determined as described previously (Bussmann et al., 2015). After filling triplicate sample bottles and one control bottle, a diluted tracer (0.1 ml of ^3H-CH_4, American Radiolabeled Chemicals) was added to the samples (2 kBq ml^{-1}). The samples were shaken vigorously and incubated for 24 hours in the dark at near in situ temperatures (approximately 4–10°C). After incubation, methane oxidation was stopped by adding 0.3 ml of 25% H_2SO_4. (Controls were stopped before the addition of the tracer.) The principle of the MOX estimation is the comparison between the total amount of radioactivity added to the water sample and the radioactive water that was produced due to oxidation of the tritiated methane. The ratio between these values, corrected for the incubation time, is the fractional turnover rate (k'; d^{-1}). The in situ MOX (nmol L^{-1} d^{-1}) is then obtained by multiplying k' with the in situ methane concentration. We also calculated the turnover time (1 /k') (i.e. the time it would take to oxidise all the methane at a given MOX, assuming that methane oxidation is a first-order reaction). The total radioactivity of the sample and the radioactivity of the tritiated water were determined by mixing 4-ml aliquots of water with 10 ml of scintillation cocktail (Ultima Gold LLT, Perkin Elmer) and analysing with a liquid scintillation counter (Beckman LS 6500). The limit of detection was calculated as described previously (Bussmann et al., 2015) and was determined to be 0.028 nmol L^{-1} d^{-1} for this data set.

2.4 PCR amplification of methane monooxygenase genes

Samples (250 ml) from surface and bottom water were filtered through 0.2 μm cellulose acetate filters (Sartorius) and stored frozen until further processing. High molecular weight DNA was extracted following the protocol of PowerWater® DNA Isolation Kit (MoBio). DNA concentrations were determined photometrically (TECAN infinite200). Each DNA sample was checked for the presence of methanotrophic DNA with the primers wcpmoA189f / wcpmoA661r, as water column-specific primers (Tavormina et al., 2008). Each PCR reaction (30 μl) contained 2 U of Taq Polymerase (5 Prime), 3 μl PCR Buffer (10×), 6 μl PCR Master Enhancer (5×), 200 μM dNTP Mix (10 mM Promega), 0.6 μM of each primer, and 10 ng of DNA template. Initial denaturation at 92 °C for 180 s was followed by 30 cycles of denaturation at 92 °C for 30 s, annealing at 59 °C for 60 s and elongation at 72 °C for 30 s. The final elongation step was at 68 °C for 300 s. Successful amplification was confirmed by gel electrophoresis on a 1.5% (w/v) agarose gel.

2.5 Quantitative PCR (qPCR) of methane monooxygenase genes

Extracted DNA from each sample was amplified by qPCR using a LightCycler R 480 (Roche, Germany) and master mixes from the company (Roche, Germany). Each sample was measured in triplicate.

A pure culture of *Methylobacter luteus* (NCIMB 11914) was used to construct standard curves for the total *pmoA* gene. Cell numbers of the *M. luteus* cultures were determined after staining with a microscope and after extraction, DNA was quantified using a TECAN infinite M200 spectrophotometer (TECAN, Switzerland). A serial dilution of DNA (equivalent to 10–10^6 cells ml^{-1}) was used to construct standard curves. Correlation coefficients of standard curves were > 0.98.

The qPCR reaction mix (20 μl) contained 10 μl Master Mix (2 × LightCycler® 480 kit hot-start SYBR Green I Master, Roche, Germany), 10 mM of each PCR-primer (as described above) and 5 μl template DNA. The amplification was performed with an initial denaturation step at 95 °C for 5 min, followed by 45 cycles of denaturation at 95 °C for 10 s, annealing at 59 °C for 60 s and extension at 72 °C for 30 s. Fluorescence data were acquired during an additional temperature step (60 s at 65 °C).

2.6 Methane monooxygenase intergenic spacer analysis (MISA)

All samples showing *pmoA* genes were analysed with MISA to differentiate the methanotrophic populations and describe their "estimated diversity" by analysing the differences in the composition of methane monooxygenase genes with regard to their geographical distribution (Tavormina et al., 2010).

The PCR master mix (20 µl) contained 200 μM dNTPs, (Promega), 2 U Taq DNA polymerase (5 Prime), 2 μl PCR Buffer (10x), 4 μl PCR Master Enhancer (5 ×), and 15 ng target DNA. Two PCR runs were carried out with a MasterCycler gradient (Eppendorf, Germany) modified after (Tavormina et al., 2010) using two sets of primers (Thermo Fisher Scientific GmbH, Germany): The *pmoA* sequences were enriched from bulk environmental DNA using primers spacer_pmoC599f (5'-AAYGARTGGGGHCAYRCBTTC), spacer_pmoA192r (5'-TCDGMCCARAARTCCCARTC). A second round of semi-nested amplification was performed using the primers spacer_pmoC626_IRD (5'-RCBTTCTGGHTBATGGAAGA) and spacer_pmoA189r (5'-CCARAARTCCCARTCNCC) and the purified PCR product from the first PCR as the template. Primer spacer_pmoC626_IRD is labelled with an infrared Dye (Dy 682 nm) for the detection of amplified products using a Licor DNA Analyser 4300 system (Licor, Germany). Primers are modified versions of MISA primers, as reported previously (Tavormina et al., 2010). Modifications used in the current work increased amplicon strength and recovery of diverged lineages (Tavormina, pers. comm.). In detail, in the first PCR, an initial denaturation at 94 °C for 180 s was followed by 30 cycles of denaturation at 94 °C for 30 s, annealing at 52 °C for 60 s and elongation at 72 °C for 30 s. The final elongation step was at 72 °C for 300 s. In the second PCR, 2 μl of purified PCR product from the first PCR was used for amplification with modified and labelled primers (see above). The PCR program was modified as follows: initial denaturation at 94 °C for 180 s was followed by 5 cycles of denaturation at 94 °C for 30 s, annealing at 52 °C for 60 s, elongation at 72 °C for 30 s and 25 cycles with an annealing temperature of 48 °C.

Amplified samples were separated on polyacrylamide gels using a DNA Analyser 4300 (Licor, Germany). Running conditions on a 6.5% polyacrylamide gel (Lonza, Switzerland, 25 cm length, 0.25 mm thickness) were

1500 Volt, 40 mA, 40 W for 3.30 h at 45 °C. A 50–700 bp sizing standard (IRDye 700, Licor, Germany) was applied to the gel. For the analysis of the MISA fingerprints (Bionumerics 7.0, Applied Maths, Belgium), size fragments of 350 to 700 bp were included (Schaal, 2016). Binning to band classes was performed with a position tolerance setting of 1.88%. Each band class is referred to as a MISA operational taxonomic unit (MISA-OTU). Band patterns of the MISA-OTUs were translated to binary data reflecting the presence or absence of the respective OTU.

2.7 Calculation of the diffusive methane flux

The gas exchange across an air–water interface can be described in general by the following function (Wanninkhof et al., 2009):

$$F = k_{CH4} * (c_m - c_{equ})$$

where F is the rate of gas flux per unit area (mol m^{-2} d^{-1}), c_m is the methane concentration measured in surface water and c_{equ} is the atmospheric gas equilibrium concentration (Wiesenburg and Guinasso, 1979). Data on the atmospheric methane concentration were obtained from the meteorological station in Tiksi via NOAA, Earth System Research Laboratory, Global Monitoring Division (http://www.esrl.noaa.gov/gmd/dv/iadv/). The gas exchange coefficient (k) is a function of water surface agitation. The k value in oceans and estuaries is determined more by wind speed, whereas water velocity dominates in rivers (Alin et al., 2011). The determination of k is very important for the calculation of the sea–air flux. We decided to calculate k_{600} in the in the Laptev Sea according to the following equation, obtained for coastal seas (Nightingale et al., 2000):

$$k_{600} = 0.333\ U_{10} + 0.222\ U_{10}^2$$

Wind data (U_{10}) were obtained for Tiksi from the "Archive of Tiksi for Standard Meteorological Observations" (Institute, 2016). The median wind speed of each day was used for the flux calculation. The calculated k_{600} (value for CO_2 at 20°C) was converted to k_{CH4} (Striegl et al., 2012), where Schmidt numbers (Sc) are determined by water temperature and salinity (Wanninkhof, 2014):

$$k_{CH4} / k_{600} = (Sc_{CH4} / Sc_{CO2})^{0.5}$$

The role of methane oxidation and the diffusive methane flux for the methane inventory in the Lena Delta were estimated using the following calculations. Two rectangles which are bordered by the most southern, northern, eastern and western stations gave a good estimation of investigated area (Figure 1). The median depth from the stations within each of these squares was 13 m. Based on the longitude / latitude of the squares, we calculated the area (1.02×10^{10} m^2 and 2.01×10^{10} m^2) and then the volume of each square (1.3×10^{11} m^3 and 2.5×10^{11} m^3). With the median methane concentration and median MOX of all stations within each square, we calculated the total methane inventory of the investigated areas (in mol, sum of both squares), as well as the total methane oxidation rate (mol / d). The total diffusive flux (in mol / d) of the region was obtained by multiplying the median diffusive flux for all stations with the total area.

2.8 Statistical analysis

We tested for differences between the different water masses by applying a one-way analysis of variance (ANOVA) with log transformed data (Kaleidagraph 4.5). We tested for differences between different groups using the non-parametric Wilcoxon or Kruskal Wallis test (Kaleidagraph 4.5). The linear correlation analyses were also performed with log transformed data and Kaleidagraph 4.5.

3 Results

3.1 Hydrography

We grouped our sampling stations into "riverine water" with a salinity < 5. In this water mass, the median salinity was 2.45, ranging from 0.8–4.8, and the median temperature was 9.8 °C, ranging from 7.3–11.4 °C. In the "mixed water", the median salinity was 11.4, ranging from 5–19.7, and the median temperature was 6.4 °C, ranging from 2.5–8.8 °C. In the "polar water", the median salinity was 27.2, ranging from 21.5–33.2, and the median temperature was 3.0 °C, ranging from 1.8–6.2 °C. In September 2013, we observed a sharp stratification, with warm freshwater at the surface (0–5 m), followed by a mixed water body. Below an approximate10 m water depth, we found cold and saline water (= "polar water"). As an example of this sharp stratification, the salinity distribution of Transect 1 is shown in Figure 2a. The freshwater plume was most pronounced in Transects 4 and 5 and extended far to the north (Appendix Figure A1). In Transect 6, only the first near-shore station had riverine water, the subsequent stations were already characterised by polar waters.

3.2 Methane concentrations

Methane around the Lena Delta showed elevated concentrations near the shore and decreased with distance from the shore (Figure 3). This decrease off the coast was most distinct for Transects 1 and 4, which also had the maximal concentrations (218 nmol L^{-1}). At station TIII-13 04, we also observed comparably high methane concentrations at the surface (212 nmol L^{-1}; Figure 3). By contrast, methane concentrations were distributed rather uniformly in the northern Transect 6. No clear pattern was observed in the depth distribution of methane (Figure 2b). Methane concentrations of the sediment surface ranged from 430 nmol L^{-1} at the eastern station of Transect 4 and 5380 nmol L^{-1} at the beginning of Transect 1 (overall median of 2070 nmol L^{-1}).

When applying our water masses (riverine, mixed and polar), we observed significantly different methane concentrations in these water masses, with medians of 22, 19 and 26 nmol L^{-1} ($p = 0.03$), respectively (Table 1). Therefore, the linear correlation analysis was performed separately for the different water masses.

In "riverine water", the methane concentration was significantly correlated with temperature ($r^2 = 0.38$, Table 2) and negatively correlated with the oxygen concentration ($r^2 = 0.73$). In "mixed water", we found a weak but significant correlation between methane and TDN ($r^2 = 0.27$, Table 2). In "polar water", the methane concentration of the water column was significantly correlated with the methane concentration in the surface sediment ($r^2 = 0.33$). The influence of the sediment methane concentration on the water column concentration was even more pronounced when taking all bottom water samples (= "polar water" + one "mixed water" + one

"riverine" sample) and excluding the very high water values of station TIII-1304; which made the correlation much stronger ($r^2 = 0.62$, n= 33, Figure 4).

3.3 Methane oxidation rate (MOX) and fractional turnover (k')

The MOX ranged from below the detection limit (< 0.028 nmol $L^{-1}d^{-1}$, with 8.7% of the data) up to 5.7 nmol L^{-1} d^{-1}. In "riverine" and "polar water", methane oxidation was rather high (median of 0.419 and 0.400 nmol L^{-1} d^{-1}) compared to the low rates in "mixed water" (median of 0.089 nmol $L^{-1}d^{-1}$,Table 1). On a spatial range, we observed slightly elevated rates near the coast, at the beginning of the Transects 1 and 4 (Figure 5a). In the bottom waters, elevated values were also observed near the coast, at the beginning of Transects 4 and 5.

In the "riverine water", the MOX was significantly correlated with temperature ($r^2 = 0.77$, Table 3). In "mixed water", none of the measured parameters was of any significance. In "polar water", TDN explained 31% of the observed MOX variability, although at a low level of significance ($p<0.1$). In all water masses, MOX was influenced by the methane concentration, but the influence was strongest in "riverine water" ($r^2 = 0.98$) and decreased towards "mixed" and "polar" water ($r^2 = 0.80$ and 0.56 respectively, Table 3). However, as MOX is calculated with the methane concentration, this correlation has to be regarded with caution.

The fractional turnover (k') is a measure of the relative activity of the MOBs, and it is independent of the methane concentration. We observed significantly different k' values in riverine, mixed and polar water, with the highest k' in "polar water" (median of 0.011, 0.006 and 0.028 d^{-1}, respectively, Table 3). Temperature was the most important parameter for the k' in riverine water ($r^2 = 0.84$). In "mixed water", salinity and TDN correlated with k' ($r^2 = 0.46$ and 0.37 respectively). In "polar water", none of our parameters was of any importance (Table 3).

3.4 Relative abundance of methane oxidising bacteria (MOB)

The abundance of MOB can either be given either in cell numbers or as relative abundance. Cell numbers ranged from 4.0×10^4 to 4.6×10^5 cells per L, except at station T1-1302, which had very high numbers of 2×10^6 to 3×10^6 cells per L. The relative abundance (relating the MOB-DNA to the total extracted DNA) ranged from 0.05 to 0.47%, except for the high values from station T1-1302 at 1.69 and 2.63% (surface and bottom, respectively, Figure 6). The detection limit was 3.2×10^4 cells / L, and about one quarter of the samples were below this limit.

The relative abundance of MOB was significantly different between riverine, mixed and polar waters (Table 1). "Riverine" water had the highest relative abundance, which then decreased towards the "polar water" (median values of 0.81, 0.19 and 0.03% respectively).

For further analysis, we excluded the outliers with their very high values, and since the total number of data points was small (n = 18), we performed a linear regression analysis with all values (no separation of the different water masses). None of the methane-related parameters (methane concentration, MOX and k') could explain the observed relative abundance of MOBs. However, the relative abundance of MOBs was significantly and positively correlated with DOC and temperature ($r^2 = 0.52$; $p = 0.0002$ and $r^2 = 0.41$; $p = 0.0002$) and negatively correlated with salinity ($r^2 = 0.47$; $p < 0.0001$). Additionally, the "estimated diversity", as OTUs per station, showed a weak but significant correlation with relative abundance ($r^2 = 0.20$; $p = 0.04$). Similar results were obtained using the cell numbers as a dependent parameter.

3.5 Methanotrophic population

The MISA fingerprinting method allowed the detection of 9 different OTUs, which we named according to their PCR fragment length (size in bp). Of these, two OTUs (420 and 506) were observed at all stations and at all depths. Thus, their occurrence pattern could not provide any ecological information and they were excluded from further analysis. The "estimated diversity" of MOBs, as number of OTUs per station, was significantly different between riverine, mixed and polar waters, with 4, 3 and 2 OTUs per station, respectively (Kruskal Wallis test, p = 0.02, Table 4Table 4). The Kruskal-Wallis test was applied for each OTU (presence / absence data) to analyse the association with the three water masses. OTU-557 showed a clear association with polar water (p =0.06), while OTU-460 and OTU-398 were absent from polar water. OTU-535 showed a significant association with river and mixed water (p=0.02), as did OTU-362 (although not statistically significant). OTU-485 and OTU-445 showed no clear association. With respect to the PCR fragment size, some of the OTUs have been described previously (Tavormina et al., 2010), thus OTU-535 could be assigned to Group Z, OTU-485 to *Methylococcus capsulatus* and *Methylohalobius crimeensis* and OTU-445 to OPU-1(Table 4).

3.6 Diffusive methane flux

Calculation of the diffusive flux of methane requires information on the atmospheric methane concentration as well as the wind speed for the respective dates, as outlined in the Material & Methods section. The atmospheric methane concentration ranged from 1.896 to 1.911 ppm CH_4. The wind speed in September 2013 was rather low, at 4.2 ± 2.2 m/s. The calculated values for k_{600} ranged from 0.37 to 3.17 m d^{-1}, with a median of 1.05 m d^{-1}, while k_{CH4} ranged from 0.52 to 4.51 m d^{-1}, with a median of 1.43 m d^{-1}.

The diffusive flux of methane into the atmosphere was rather low for the Transects 1, 5 and 6, with median values of 31, 8 and 13 μmol m^{-2} d^{-1}, respectively, compared to a median flux of 163 μmol m^{-2} d^{-1} for Transect 4. The highest flux was observed at the near shore stations of Transect 4, at 478 and 593 μmol m^{-2} d^{-1}; this was mainly due to higher methane concentrations (118 and 151 nmol L^{-1}) and higher wind speeds on the sampling day.

Our cruise covered a total area of 3051 km^2 (Figure 1), with an inventory of 10161 kmol methane. Based on our estimations, about 822 kmol per day (the median value of all stations) diffused into the atmosphere, while 118 kmol per day (the median value of all stations) were oxidised. Thus, about 8% of the total methane inventory leaves the aquatic system via diffusion, while only 1% was oxidised each day.

4 Discussion

4.1 Methane concentrations

In the coastal area of the Laptev Sea, we observed rather low methane concentrations (overall median 25 nmol L^{-1}, ranging from 10 to 218 nmol L^{-1}). Transect 1 was located at the same positions as in our expedition in 2010 (Bussmann, 2013a). Near the shore, methane concentrations were slightly higher in 2013, but overall, there was

no significant difference (Wilcoxon Rank Sign Test for paired data, n = 18, p = 0.84). In the same study area and in the summer of 2014, other authors reported a range of 10 to 100 nmol L^{-1} (estimated from Figure 2 in (Sapart et al., 2017). For other arctic estuaries, namely Ob and Yenisei, similar low concentrations were reported: 18 ± 16 nmol L^{-1} by Savvichev et al. (2010) and approx. 30 nmol L^{-1} by Kodina et al. (2008). Near the Alaskan coast, up to 20 water depth maximal concentrations of 50 nM have been reported (Lorenson et al., 2016). Thus, our methane concentration lay well within the range of other arctic river and coastal systems. A more detailed comparison with temperate and tropical environments is discussed below, in the context of the diffusive methane flux, as most reviews rely on the methane emissions rather than on the concentrations.

The water masses we had classified were separated by a strong pycnocline. Thus, different parameters also influenced the corresponding methane distribution. In polar water, with a median methane concentration of 26 nmol L^{-1}, linear regression analysis revealed the methane concentrations of the surface sediments as the only important factor determining the methane concentration in the water above. Thus, we assume that this methane mostly originates from a methane flux out of the sediment. In the shallow Chucki Sea, the most likely methane source was also seafloor methanogenesis resulting from the decomposition of organic carbon (Fenwick et al.; 2017). Another source of methane for bottom waters is submarine groundwater discharge, as shown for two Alaskan sites (Lecher et al., 2016). However, low tides, low topographic relief and low precipitation in the present study area are not favourable for a high ground water input to the Lena Delta. Highly active methane seeps are also reported for this region (Shakhova et al., 2014), and methane ebullition could also be a reason for the observed high methane concentrations. No sonar data were available for our cruise, so we do not have any information on seep activity. In addition, our data do not show an increased methane concentration at the pycnocline, where entrapped gas bubbles could dissolve (Gentz et al., 2013). Thus, we cannot support ebullition as a methane source. However, no isotope analysis was possible to verify the origin of the bottom water methane.

In riverine water, at the surface, several methane sources are possible: in situ production, input from bottom water and riverine input. We showed that the methane concentrations in riverine water were correlated positively with temperature and negatively with oxygen concentration. This correlation could be related to degradation processes that ultimately lead to methanogenesis, as these processes are enhanced by temperature and are oxygen consuming. The removal of DOM occurs primarily at the surface layer, where about 50% of the terrestrial organic material is mineralised (Kaiser et al., 2017). For lakes and oceans, a link between methane production and photosynthesis (Tang et al., 2014), or even evidence of methane production by marine algae (Lenhart et al., 2016), is reported, resulting in oversaturated methane concentrations in surface waters. Dimethylsulphoniopropionate (DMSP) as an osmoprotectant and antioxidant in microalgae could also lead to in situ methane production (Florez-Leiva et al., 2013). However, for the latter two processes, it not clear yet if this methane production will result in elevated methane concentrations in situ.

Methane input from bottom water to surface water will not be important at the deeper stations, e.g. T1-1304 - 07, a strong water column stratification will limit any exchanges processes. However, at the shallow stations (< 8 m, coastal stations of the transects), the water column was mixed; thus, sedimentary methane may diffuse into the water above.

Another source of methane might be the water of the Lena River itself, as rivers or estuaries are thought to import methane-rich water into coastal seas. Methane concentrations in the Bykowski Channel of the Lena River are, on average, 58 ± 19 nmol L^{-1} (Bussmann 2013 and unpublished data from 2012 and 2016). We did find elevated methane concentrations near the coast; however, no correlation was evident between salinity and methane concentration (i.e. no dilution of methane-rich river water with methane-poor marine water was observed) either for the separate water masses or for the whole data set, Figure 7. This is also confirmed by our previous study (Bussmann, 2013a). For other estuaries, a complex pattern of increasing/decreasing methane concentrations versus salinity has been presented (Borges and Abril, 2012). However, even this scheme does not seem applicable to our data.

One reason for the lack of significant correlation could be another source of freshwater, but with minor methane concentrations. In contrast to other estuaries, arctic estuaries are ice covered for about two thirds of the year, and the seasonal freezing and melting of ice has a strong impact on the water budget. The freezing of sea water results in brine formation with strongly increased salinity, while its melting results in a freshwater input (Eicken et al., 2005). To a lesser extent, this also holds true for freshwater ice. In 1999, the river water fraction in ice-cores near our study area ranged from 57 to 88% (Eicken et al., 2005). Thus, when this ice melts in spring, we expect an additional non-river-freshwater input. Even though not much is known about methane concentrations in ice, based on a recent study on sea-ice in the East Siberian Sea (Damm et al., 2015), we assume that this melt water probably has lower methane concentrations than the river freshwater. The melting of ice in springtime thus results in a freshwater input with a minor methane concentration compared to river water with higher methane concentrations. This additional aspect of the water budget in ice-covered estuaries might explain the missing relationship between salinity and methane concentration in the Lena Delta.

4.2 Methanotrophic activity and the methanotrophic population

We measured an overall median methane oxidation rate of 0.32 nmol L^{-1} d^{-1}, ranging from 0.03 to 5.7. In other coastal seas, comparable values were observed, with a median of 0.82 and 0.16 nmol L^{-1} d^{-1} for the coastal and marine parts of the North Sea, respectively (Osudar et al., 2015), 0.1 nmol L^{-1} d^{-1} at the surface of the central North Sea (Mau et al., 2015) and 1 to 11 nmol L^{-1} d^{-1} for Eckernförde Bay in the Baltic Sea (Steinle et al., 2017). In polar waters, off Svalbard and unaffected from ebullition sites, values of 0.26 to 0.68 nmol L^{-1} d^{-1} (Mau et al., 2017) and 0.5 ± 1 nmol L^{-1} d^{-1} (Steinle et al., 2015) are reported. Thus, our values are well within the reported range of coastal and polar MOX. However, at the source of the "riverine water" (i.e. the Lena River itself), much higher MOX (median = 24 nmol L^{-1} d^{-1}) have been observed (Osudar et al., 2016). The first order rate constant used for modelling the methane flux in the Laptev Sea is estimated to range from 18116 d^{-1} to 11 d^{-1} (= 2.3×10^{-6} to 3.8×10^{-3} h^{-1}) (Wahlström and Meier, 2014). Based on our data, we suggest more realistic first order constants (and turnover times) of 0.01 d^{-1} (91 d) in riverine water, 0.006 d^{-1} (167 d) in the mixed water and 0.03 d^{-1} (36 d)$^{-}$ in polar water.

In the "riverine water", MOX and fractional turnover rates were correlated with temperature (ranging from 7 to 11°C), while in the other water masses, no such correlation was found. The influence of the methane concentration on the MOX was also most pronounced in "riverine water" ($r^2 = 0.98$). In polar water, methane concentration had a much lower influence ($r^2 = 0.56$).

With the described method of qPCR and the water column specific primers (Tavormina et al., 2008), the relative abundance of MOB in our study ranged from 0.05 to 0.47% (median 0.16%) which is equivalent to 4×10^4 to 3×10^6 cells per L (median of 6.3×10^4), except for the high values from station T1-1302. These high values could not be explained by any environmental or methane-related parameters; thus, they are regarded as methodological outliers. In a marine non-methane-seep area, 2 to 90 copies of MOB-DNA per ml, equivalent to 1 to 45×10^3 cells/L, are reported (Tavormina et al., 2010), assuming two copies of the pmoA gene per cell (Kolb et al., 2003). In the Lena River, the number of MOB ranges from 1–8×10^3 cells / L (Osudar et al., 2016). In the boreal North Sea, a broad range of 0.2×10^3 to 8×10^8 cells/L were found (Hackbusch, 2014). These studies all had used qPCR with the same primers as used here. Thus, our numbers are within the upper range of the reported values. When using CARD-FISH, the number of MOB seem to be higher, with 3 to 30×10^6 MOB cells/L in polar waters off Svalbard (Steinle et al., 2015) and 1×10^6 cells/L at surface waters at the Coal Oil Point seep field in California (Schmale et al., 2015).

We found no correlation for either cell numbers or relative abundance of MOB and methane-related parameters (methane concentration, MOX and k'), but found correlations between parameters important to heterotrophic bacteria, such as the amount of organic carbon, temperature and salinity (Lucas et al., 2016). Thus, we have to assume that our qPCR also detected cells that were not active. This is supported by the finding that even when MOX was not detectable, we still detected MOB-DNA in our samples. Vice versa, when MOB-DNA was not detectable, we still could measure their activity (MOX). This could be due to the fact that there are MOB which were probably not amplified. The primer set used in this study is the most frequently used; however, a couple of different primer sets are available for amplification of specific monooxygenase genes in several subgroups which are not targeted using this primer set (Knief, 2015). Thus, these subgroups – for example, *Verrucomicrobia* or the anaerobic methanotrophic bacteria of the NC10 phylum, and others (Knief, 2015) – were not quantified in our study. Additionally, dormant MOB might be present, whose DNA we detected even though the cells were not active (Krause et al., 2012). Thus, we can state that the different water masses had significantly different abundances of MOB, with the highest abundance in "riverine water" and the lowest abundance in "polar water".

The use of the MISA method in the present study allowed the first successful fingerprinting of the methanotrophic population in a polar estuary. However until now, only one study has applied MISA to environmental samples at present, and two OTUs have been described in that marine study (Tavormina et al., 2010). The first group, OTU-1 has a broad distribution and belongs to the known group of gammaproteobacteria. OTU-445, assigned to group OTU-1, was distributed equally in all the different water masses we analysed. Group-Z is described as being not so abundant and belongs to a group of MOB of unknown lineage and function (Tavormina et al., 2010). In the present study, OTU-535, which was assigned to the Group-Z, preferred the non-polar environment. OTU-485, which is assigned to the group of *Methylococcus*, showed no specific association. Thus, we conclude that the methanotrophic populations differ in polar versus river/mixed water, with some OTUs not occurring in polar water and one OTU with a clear association with polar water. The populations in riverine and mixed water were very similar. Since a subset of OTUs identified in this study cannot be linked to known MOB, further attempts to isolate and describe new unknown polar MOB would be helpful to learn more about the diversity and the potential of these MOB, but this is a challenging task. Further insight could also be obtained by next-generation sequencing, which gives an in depth view of population structure. Meta-genome and

meta-transcriptome analyses could also help to identify functional genes and reveal which types are really active and which are dormant.

Thus, the ecological traits can be described as follows: we observed two distinct methanotrophic populations with different characteristic in the riverine versus polar water mass. In polar water, the methanotrophic activity was influenced by the nitrogen content and scarcely by the methane concentration. The relative abundance and "estimated diversity" (OTU/sample) of MOB was lower in polar water than in riverine water. Thus, this polar population was well adapted to the cold and methane-poor environment, but limited by the nitrogen content. With their lower relative abundance and lower "estimated diversity", the MOB in the polar population were quite efficient at reaching a MOX comparable to riverine water. In the riverine water, the methanotrophic activity was limited by temperature and methane concentrations. The relative abundance and "estimated diversity" (OTU/sample) of MOB was higher in riverine water than in polar water, even though the same MOX was measured. Thus, this riverine population was not very efficient at sub-optimal temperatures and substrate concentrations.

Methane concentration and nitrogen availability are strong driving forces shaping MOB community composition and activity (Ho et al., 2013). Furthermore the interactions with other heterotrophic bacteria influence the methanotrophic community (Ho et al., 2014). As DOM removal and degradation occurs mainly at the surface / riverine water (Gonçalves-Araujo et al., 2015), this may also lead to an enriched methanotrophic population in the riverine water. We also assume that the riverine environment is subject to more environmental changes (salinity, light, temperature) when compared to the polar one. Changes in salinity have different impacts on sensitive and non-sensitive MOBs, thereby shaping the methanotrophic community (Osudar et al., accepted). In contrast to our more diverse riverine population, the methanotrophic population in the Lena River proper was characterised by a rather homogenous community (Osudar et al., 2016). However, the classical concept of the r- and k-strategist has today been replaced by the C-S-R functional classification framework. Thus, the type Ia MOB, which respond rapidly to substrate availability and are the predominant active community in many environments, can thus be classified as competitors (C) and competitors-ruderals (C-R) (Ho et al., 2013).

4.3 Diffusive methane flux

The calculation of the diffusive methane flux requires several parameters, including the atmospheric methane concentrations which, as obtained from the database, ranged from 1.896 to 1.911 ppm. This is within the range of previously reported values for the outer ice free Laptev Sea in summer 2014 (1.879 ppm, Thornton et al., 2016). By contrast, our wind speed was somewhat higher (4.2 ± 2.2 m/s) than the 2.9 ± 1.9 m/s reported previously (Thornton et al., 2016). This would result in slightly higher equilibrium concentrations and higher gas exchange coefficient in our study.

The gas exchange coefficient is more critical and also more difficult to assess. No current method is totally satisfactory for quantifying k in estuaries, and this remains a matter of debate (Borges and Abril, 2012). In their review, Borges & Abril report an approximate range for k_{600} of < 10 up to 30 cm/h (< 2.4–7.2 m/d). For the North Sea in winter much higher values are given (7–62 cm/h = 17–150 m/d) (Nightingale et al., 2000). Similar values are given for a Bay in the Baltic Sea, at around 7 cm/h = 17 m/d (Silvennoinen et al., 2008), but lower values are reported for a Japanese estuary in summer (0.69–3.2 cm/h = 1.7 -7.7 m/d) (Tokoro et al., 2007). Our

values for k_{600} ranged from 0.37 to 3.17 m d^{-1}, with a median of 1.05 m d^{-1}. Thus, our k_{600} values lay within the lower range reported in the literature.

With all the assumptions and additional data, we calculated a median diffusive methane flux of 24 μmol m^2 d^{-1}, ranging from 4–163 μmol m^2 d^{-1}. Our data lay well within the range of data reported from previous studies within this area (Table 5Table 5) (Bussmann, 2013a;Shakhova and Semiletov, 2007). (Wahlström and Meier, 2014) applied a modelling approach that resulted in even lower methane fluxes (Table 5). The area off Svalbard is another polar region with an appreciable scientific focus. A comprehensive study by (Myhre et al., 2016) calculated a median methane flux of only 3 μmol m^2 d^{-1}, which is supported by a median methane flux of 2 μmol m^2 d^{-1} for the coastal waters of Svalbard (Mau et al., 2017) and lies within the previously reported range of 4–20 μmol m^2 d^{-1} (Graves et al., 2015) (Table 5Table 5). For the North American Arctic Ocean and its shelf seas, rather low methane fluxes are reported (1.3 μmol m^2 d^{-1}) (Fenwick et al. 2017).

Our two stations with the high methane fluxes have values similar to those reported for the North Sea with a mixed water column. In the North Sea, the stratification of the water column in the summer significantly reduced the diffusive methane flux, even at an active seep location (Mau et al., 2015). For a stratified Fjord in the Baltic Sea, the values are comparable to those of the North Sea (Steinle et al. 2017). However, in the southern North Sea, with a mixed water column, very high methane fluxes (> 200 μmol m^2 d^{-1}) are reported which are mainly related to organic-rich sediments (Borges et al., 2016). A summary study of European estuaries reported an average methane emission of 118 μmol m^2 d^{-1} (Upstill-Goddard and Barnes, 2016).

Table 5 shows a comparison of our methane emission rates with those from other polar sites, as well as some temperate ones. Methane emission in polar sites seems a bit lower than that in temperate ones; however, even within the polar environments a broad range of emission data occurs. A worldwide comparison of riverine and aquatic methane emissions is presented by (Stanley et al., 2016) and (Ortiz-Llorente and Alvarez-Cobelas, 2012). Both studies reveal no correlation between methane emissions and latitude, in contrast to the review by (Borges and Abril, 2012) comparing worldwide estuaries. In that study, an increase in methane emissions was evident from the higher latitudes, as well as from tidal systems, to which the Lena Delta would be classified. No overall pattern of controlling factors of methane emission were revealed by (Ortiz-Llorente and Alvarez-Cobelas, 2012); thus, they concluded that local studies are vital for assessing methane emission and its controlling factors. The presence and strength of a pycnocline is especially critical. Environments without stratification will emit much more methane (Borges et al., 2017) than will stratified systems where methane oxidation can consume part of the methane (Mau et al., 2015). Temperature is another important environmental control factor. Methane production is very temperature sensitive (i.e. methanogenesis is higher at higher temperatures), so one would expect higher methane concentrations and emissions in tropical and temperate regions (Borges et al., 2017;Lofton et al., 2014) and lower concentrations and emissions in polar areas. However, methane oxidation is less influenced by temperature, so this may offset methane consumption versus methane production in polar areas (Lofton et al., 2014), thereby resulting in overall lower methane concentrations in polar regions. In addition, the influence of thawing permafrost on the polar methane cycle is controversial (Overduin et al., 2015;Shakhova et al., 2010). A molecular approach identified the salinity, temperature and pH as the most important environmental drivers of methanogenic community composition on a global scale. However, how changes in these factors will influence the methanogenesis rate remains elusive, owing to a lack of studies that combine methane production rates with community analyses (Wen et al., 2017).

In contrast to these bottom-up calculations, very few studies have focused on the atmospheric methane concentrations in this area (Thornton et al., 2016;Shakhova et al., 2014;Shakhova et al., 2010) or in polar regions (Myhre et al., 2016). The resulting top-down calculations of the methane flux seem to be higher than the bottom-up calculations, at 94 and 200–300 μmol m^2 d^{-1}, respectively (Thornton et al., 2016;Myhre et al., 2016). Ebullition of methane from the sediment in this area is also reported, resulting in very high methane fluxes that are 1–2 orders of magnitude higher than the other calculations

). The methane released by ebullition did not show any isotopic evidence of oxidation; thus, it will be released almost completely into the atmosphere (Sapart et al. 2017). However, whether this ebullition really results in elevated atmospheric methane concentrations remains a matter of debate, as this fingerprint was not detected by others (Thornton et al., 2016;Berchet et al., 2015). Overall, the East Siberian Arctic shelf seems to play an insignificant role in the methane emissions, when compared to wetland and anthropogenic methane emissions in eastern Siberia (Berchet et al., 2015).

4.4 Role of microbial methane oxidation versus diffusive methane flux

We estimated the role of methane oxidation and diffusive methane flux for the methane inventory in the Lena Delta by calculating the total methane inventory (for details, see the Method section), as well as the total methane oxidation and total diffusive flux of this area. When the total methane inventory was set to 100%, then a median of 1% (range 0.3–3.8%) was consumed within one day by bacteria within the system, while a median of 8% (1–47%) left the system into the atmosphere. A similar estimation has been made (Mau et al., 2017) for the coastal waters of Svalbard, where a much higher fraction of the dissolved methane (0.02-7.7%) was oxidised and only a minor fraction (0.07%) was transferred into the atmosphere. However, this region was much deeper; thus, the ratio of water volume (including the methane oxidation activity) to the surface area (including the diffusive methane flux) was much larger. Another polar study off Svalbard suggests that about 60% of the methane in the bottom water is oxidised before it can mix with intermediate or surface water (Graves et al., 2015). For the coastal waters of the Baltic Sea, the given values for total MOX and total diffusive flux were related to the total methane inventory. Accordingly, with a weakly or strongly stratified water column, about 1.5 to 3.5% of the methane inventory was oxidised, while 0.2 to 5.2% diffused into the atmosphere, respectively (Steinle et al. 2017).

However, one fact to be kept in mind is that our estimation is a static one and does not take into account the currents and spreading of the freshwater plume. In estuaries, the residence time of the water (as influenced by water discharge and tidal force) also influences the efficiency of the estuarine filter (Bauer et al., 2013). The bulk of the freshwater from the Lena River stays in the eastern Laptev during the summer season (Fofonova et al., 2015). However, changing atmospheric conditions render the Laptev Sea Shelf highly time-dependent and turbulent (Heim et al., 2014). A more complex approach is taken by (Wahlström and Meier, 2014). Their simulations revealed the importance of the oxidation rate constant and the crucial necessity of performing in situ measurement of the oxidation rate constant. Beside the methane oxidation rate, the concentration of methane in the river runoff and the methane flux from the sediment are statistically significant important factors for the sea-air flux of methane (Wahlström and Meier, 2014).

Conclusions

In the context of the expected and ongoing warming of the Arctic regions, two main factors will change for coastal arctic seas. A different hydrographic regime (i.e. more freshwater input and stronger stratification) is expected (Bring et al., 2016). Thawing permafrost will result in increasing fluxes of carbon and nutrients being transported into the coastal arctic. The released material will: i) directly be degraded into greenhouse gases, (ii) fuel marine primary production, (iii) be buried in nearshore sediments or (iv) be transported offshore (Fritz et al., 2017). Based on our data, we propose the following for the methane cycle in the Lena Delta:

An increased freshwater input will not necessarily lead to higher methane concentrations in the study area, as no direct dilution of riverine methane occurs; however, a more complex pattern of methane input will develop. Changes in photosynthesis remain a matter of debate, as more nutrients would be beneficial, in contrast to more turbid waters and subsequent light limitation. The effect on methane production in surface riverine water is therefore ambiguous. However, the methanotrophic population in this water mass is very diverse and will be able to adjust to a changing environment and respond well to increasing water temperatures.

A strong stratification, together with increased inputs of particulate organic material to the polar bottom water, would probably result in increased degradation processes and increased methane concentrations in the surface sediment and the water column above. The polar methanotrophic population proved to be quite efficient in our study; thus, we propose that it will compensate for any increase in methane concentrations. However, if the storm frequency/strength also increases, then the stratification of the water column will be broken up and the separate water masses mixed. In our study, we showed that conditions in the mixed water mass were not favourable for MOB, and this would lead to an approximately 4-fold reduction in MOX. An increase in methane emissions after a storm has already been shown for the study area (Shakhova et al., 2014).

In the present situation, the methane sinks in the water column of the Lena Delta were rather weak, so 1% of the methane inventory is oxidised per day and 8% diffuses into the atmosphere. Thus, these water masses represent a strong methane source for the waters of the Laptev Sea and the central Arctic Ocean, but they serve only to a limited extent as a methane source to the atmosphere.

Acknowledgments

The authors acknowledge the Captain and the crew of the R/V “Dalnie Zelentsy”. We are thankful to the logistics department of the Alfred Wegener Institute, particularly W. Schneider. Special thanks go to N. Kasatkina and D. Moiseev from the Murmansk Marine Biological Institute for offering laboratory support. We also want to thank Ellen Damm for fruitful discussions and Patricia Tavormina for help in setting up the MISA. The methane related data set is available at www.pangaea.de, doi:10.1594/PANGAEA.868494, 2016.

Figures and Tables

Figure 1. Map of the study area in September 2013 and sampling locations, with four transects heading from near shore to offshore. The dashed lines delineate the area used for the budget calculation.

Figure 2. Salinity (A) and methane (B, in nmol L^{-1}) distributions versus depth and distance from the shore for Transect 1. In (A) the water masses are also indicated, defined as "riverine" with a salinity < 5, "mixed water" with a salinity between 5 and 20, and "polar water" with a salinity > 20. The grey bars indicate the location of the stations. In (B), for stations with very high methane concentrations, the values are annotated in the figure.

Figure 3. Methane concentrations in nmol L^{-1} at the surface of the study area. For stations with very high methane concentrations, the values are annotated in the figure.

Figure 4. Correlation between the methane concentration in bottom water and the concentration in the underlying sediment for all stations ($r^2 = 0.62$, $p < 0.001$, n= 33). Two very high values from station TIII-1304 were excluded from the analysis.

Figure 5. Logarithm of the methane oxidation rates in nmol L^{-1} d^{-1} in surface (A) and bottom (B) water around the Lena Delta.

Figure 6. Relative abundance of methanotrophic DNA (as %MOB-DNA) in surface (A) and bottom (B) water around the Lena Delta. For stations with very high methane concentrations, the values are annotated in the figure.

Figure 7. Methane concentration versus salinity for riverine water (open circles), mixed water (diamonds) and polar water (open squares). The dotted line indicates a regression line for all data points ($r^2 = 0.01$, $p = 0.7$, n = 99).

Appendix Figure A1. Salinity in surface waters around the Lena Delta.

.

References

Alin, S. R., de Fátima F. L. Rasera, M., Salimon, C. I., Richey, J. E., Holtgrieve, G. W., Krusche, A. V., and Snidvongs, A.: Physical controls on carbon dioxide transfer velocity and flux in low-gradient river systems and implications for regional carbon budgets, Journal of Geophysical Research G: Biogeosci., 116, G01009, doi:10.1029/2010jg001398, 2011.

Berchet, A., Pison, I., Chevallier, F., Paris, J. D., Bousquet, P., Bonne, J. L., Arshinov, M. Y., Belan, B. D., Cressot, C., Davydov, D. K., Dlugokencky, E. J., Fofonov, A. V., Galanin, A., Lavrič, J., Machida, T., Parker, R., Sasakawa, M., Spahni, R., Stocker, B. D., and Winderlich, J.: Natural and anthropogenic methane fluxes in Eurasia: a mesoscale quantification by generalized atmospheric inversion, Biogeosci., 12, 5393-5414, doi:10.5194/bg-12-5393-2015, 2015.

Borges, A. V., and Abril, G.: Carbon Dioxide and Methane Dynamics in Estuaries, in: Treatise on estuarine and coastal science, edited by: Wolanski E, and DS, M., Academic Press, Waltham, 119–161, 2012.

Borges, A. V., Champenois, W., Gypens, N., Delille, B., and Harlay, J.: Massive marine methane emissions from near-shore shallow coastal areas, Scientific Reports, 6, 27908, 10.1038/srep27908, 2016.

Borges, A. V., Speeckaert, G. l., Champenois, W., Scranton, M. I., and Gypens, N.: Productivity and temperature as drivers of seasonal and spatial variations of dissolved methane in the Southern Bight of the North Sea, Ecosystems, doi: 10.1007/s10021-017-0171-7, 2017.

Bussmann, I.: Distribution of Methane in the Lena Delta and Buor Khaya Bay, Russia, Biogeosci., 10, 4641–4465, doi:10.5194/bg-10-4641-2013, 2013a.

Bussmann, I., Matousu, A., Osudar, R., and Mau, S.: Assessment of the radio ^{3}H-CH_4 tracer technique to measure aerobic methane oxidation in the water column Limnol. Oceanogr.: Methods, 13, 312-327, doi:10.1002/lom3.10027, 2015.

Caspers, H.: Vorschläge einer Brackwassernomenklatur (The Venice System), Int. Rev. Ges. Hydrbiol., 44, 313-316, 1959.

Damm, E., Rudels, B., Schauer, U., Mau, S., and Dieckmann, G.: Methane excess in Arctic surface water-triggered by sea ice formation and melting, Scientific Reports, 5, 16179, doi:10.1038/srep16179, 2015.

Eicken, H., Dmitrenko, I., Tyshko, K., Darovskikh, A., Dierking, W., Blahak, U., Groves, J., and Kassens, H.: Zonation of the Laptev Sea landfast ice cover and its importance in a frozen estuary, Global Planet. Change, 48, 55-83, doi.org/10.1016/j.gloplacha.2004.12.005, 2005.

Florez-Leiva, L., Damm, E., and Farías, L.: Methane production induced by dimethylsulfide in surface water of an upwelling ecosystem, Prog. Oceanogr., 112–113, 38–48, 2013.

Fofonova, V., Danilov, S., Androsov, A., Janout, M., Bauer, M., Overduin, P., Itkin, P., and Wiltshire, K. H.: Impact of wind and tides on the Lena River freshwater plume dynamics in the summer season, Ocean Dynamics, 65, 951-968, doi:10.1007/s10236-015-0847-5, 2015.

Fritz, M., Vonk, J. E., and Lantuit, H.: Collapsing Arctic coastlines, Nature Clim. Change, 7, 6-7, 10.1038/nclimate3188, 2017.

Gentz, T., Damm, E., von Deimling, J. S., Mau, S., McGinnis, D. F., and Schlüter, M.: A water column study of methane around gas flares located at the West Spitsbergen continental margin, Cont. Shelf Res., doi:10.1016/j.csr.2013.07.013, 2013.

Gonçalves-Araujo, R., Stedmon, C. A., Heim, B., Dubinenkov, I., Kraberg, A., Moiseev, D., and Bracher, A.: From fresh to marine waters: characterization and fate of dissolved organic matter in the Lena River delta region, Siberia, Frontiers in Marine Science, 2, 2015.

Graves, C. A., Steinle, L., Rehder, G., Niemann, H., Connelly, D. P., Lowry, D., Fisher, R. E., Stott, A. W., Sahling, H., and James, R. H.: Fluxes and fate of dissolved methane released at the seafloor at the landward limit of the gas hydrate stability zone offshore western Svalbard, J.Geophys. Res.: Oceans, n/a-n/a, doi:10.1002/2015JC011084, 2015.

Hackbusch, S.: Abundance and activity of methane oxidizing bacteria in the River Elbe Estuary, Master thesis, Friedrich Schiller Universität Jena, 2014.

Heim, B., Abramova, E., Doerffer, R., Günther, F., Hölemann, J., Kraberg, A., Lantuit, H., Loginova, A., Martynov, F., Overduin, P. P., and Wegner, C.: Ocean colour remote sensing in the southern Laptev Sea: evaluation and applications, Biogeosci., 11, 4191-4210, 10.5194/bg-11-4191-2014, 2014.

Ho, A., Kerckhof, F. M., Luke, C., Reim, A., Krause, S., Boon, N., and Bodelier, P. L. E.: Conceptualizing functional traits and ecological characteristics of methane-oxidizing bacteria as life strategies, Environ. Microbiol. Rep., 5, 335-345, 10.1111/j.1758-2229.2012.00370.x, 2013.

Ho, A., de Roy, K., Thas, O., De Neve, J., Hoefman, S., Vandamme, P., Heylen, K., and Boon, N.: The more, the merrier: heterotroph richness stimulates methanotrophic activity, ISME J, 8, 1945-1948, 10.1038/ismej.2014.74, 2014.

Kaiser, K., Benner, R., and Amon, R. M. W.: The fate of terrigenous dissolved organic carbon on the Eurasian shelves and export to the North Atlantic, J. Geophys. Res.: Oceans, 122, 4-22, 10.1002/2016JC012380, 2017.

Kirschke, S., Bousquet, P., Ciais, P., Saunois, M., Canadell, J. G., Dlugokencky, E. J., Bergamaschi, P., Bergmann, D., Blake, D. R., Bruhwiler, L., Cameron-Smith, P., Castaldi, S., Chevallier, F., Feng, L., Fraser, A., Heimann, M., Hodson, E. L., Houweling, S., Josse, B., Fraser, P. J., Krummel, P. B., Lamarque, J. F., Langenfelds, R. L., Le Qu√©r√©, C., Naik, V., O'Doherty, S., Palmer, P. I., Pison, I., Plummer, D., Poulter, B., Prinn, R. G., Rigby, M., Ringeval, B., Santini, M., Schmidt, M., Shindell, D. T., Simpson, I. J., Spahni, R., Steele, L. P., Strode, S. A., Sudo, K., Szopa, S., Van Der Werf, G. R., Voulgarakis, A., Van Weele, M., Weiss, R. F., Williams, J. E., and Zeng, G.: Three decades of global methane sources and sinks, Nature Geosci., 6, 813-823, 2013.

Knief, C.: Diversity and habitat preferences of cultivated and uncultivated aerobic methanotrophic bacteria evaluated based on pmoA as molecular marker, Frontiers in Microbiology, 6, 1346, doi:10.3389/fmicb.2015.01346, 2015.

Kolb, S., Knief, C., Stubner, S., and Conrad, R.: Quantitative detection of methanotrophs in soil by novel pmoA-Targeted real-time PCR assays, Appl. Environ. Microbiol., 69, 2423-2429, 2003.

Krause, S., Lüke, C., and Frenzel, P.: Methane source strength and energy flow shape methanotrophic communities in oxygen-methane counter-gradients, Environmental Microbiology Reports, 4, 203-208, doi:10.1111/j.1758-2229.2011.00322.x, 2012.

Lammers, R. B., Shiklomanov, A. I., Vörösmarty, C. J., Fekete, B. M., and Peterson, B. J.: Assessment of contemporary Arctic river runoff based on observational discharge records, J. Geophys. Res., 106(D4), 3321–3334, 2001.

Lecher, A. L., Kessler, J., Sparrow, K., Garcia-Tigreros Kodovska, F., Dimova, N., Murray, J., Tulaczyk, S., and Paytan, A.: Methane transport through submarine groundwater discharge to the North Pacific and Arctic Ocean at two Alaskan sites, Limnol. Oceanogr., 61, S344-S355, 10.1002/lno.10118, 2016.

Lenhart, K., Klintzsch, T., Langer, G., Nehrke, G., Bunge, M., Schnell, S., and Keppler, F.: Evidence for methane production by the marine algae Emiliania huxleyi, Biogeosci., 13, 3163-3174, doi:10.5194/bg-13-3163-2016, 2016.

Lofton, D., Whalen, S., and Hershey, A.: Effect of temperature on methane dynamics and evaluation of methane oxidation kinetics in shallow Arctic Alaskan lakes, Hydrobiologia, 721, 209-222, doi:10.1007/s10750-013-1663-x, 2014.

Lorenson, T. D., Greinert, J., and Coffin, R. B.: Dissolved methane in the Beaufort Sea and the Arctic Ocean, 1992–2009; sources and atmospheric flux, Limnol. Oceanogr., 61, S300-S323, 10.1002/lno.10457, 2016.

Lucas, J., Wichels, A., and Gerdts, G.: Spatiotemporal variation of the bacterioplankton community in the German Bight: from estuarine to offshore regions, Helgol. Mar. Res., doi 10.1186/s10152-016-0464-9, 2016.

Magen, C., Lapham, L. L., Pohlman, J. W., Marshall, K., Bosman, S., Casso, M., and Chanton, J. P.: A simple headspace equilibration method for measuring dissolved methane, Limnol. Oceanogr.: Methods, 12, 637-650, doi:10.4319/lom.2014.12.637, 2014.

Mau, S., Gentz, T., Körber, J. H., Torres, M. E., Römer, M., Sahling, H., Wintersteller, P., Martinez, R., Schlüter, M., and Helmke, E.: Seasonal methane accumulation and release from a gas emission site in the central North Sea, Biogeosci., 12, 5261-5276, doi:10.5194/bg-12-5261-2015, 2015.

Mau, S., Römer, M., Torres, M. E., Bussmann, I., Pape, T., Damm, E., Geprägs, P., Wintersteller, P., Hsu, C. W., Loher, M., and Bohrmann, G.: Widespread methane seepage along the continental margin off Svalbard - from Bjørnøya to Kongsfjorden, Scientific Reports, 7, 42997, 10.1038/srep42997 http://www.nature.com/articles/srep42997#supplementary-information, 2017.

Murrell, J. C., and Jetten, M. S. M.: The microbial methane cycle, Environmental Microbiology Reports, 1, 279-284, 10.1111/j.1758-2229.2009.00089.x, 2009.

Myhre, C. L., Ferré, B., Platt, S. M., Silyakova, A., Hermansen, O., Allen, G., Pisso, I., Schmidbauer, N., Stohl, A., Pitt, J., Jansson, P., Greinert, J., Percival, C., Fjaeraa, A. M., O'Shea, S. J., Gallagher, M., Breton, M. L., Bower, K. N., Bauguitte, S. J. B., Dalsøren, S., Vadakkepuliyambatta, S., Fisher, R. E., Nisbet, E. G., Lowry, D., G.Myhre, Pyle, A., Cain, M., and Mienert, J.: Extensive release of methane from Arctic seabed west of Svalbard during summer 2014 does not influence the atmosphere, Geophys. Res. Lett., 43, 4624–4631, doi:10.1002/2016GL068999, 2016.

Nightingale, P. D., Malin, G., Law, C. S., Watson, A. J., Liss, P. S., Liddicoat, M. I., Boutin, J., and Upstill-Goddard, R. C.: In situ evaluation of air-sea gas exchange parameterizations using novel conservative and volatile tracers, Glob. Biogeochem. Cycl., 14, 373-387, doi:10.1029/1999GB900091, 2000.

Nisbet, E. G., Dlugokencky, E. J., and Bousquet, P.: Methane on the rise - Again, Science, 343, 493-495, doi:10.1126/science.1247828, 2014.

Ortiz-Llorente, M. J., and Alvarez-Cobelas, M.: Comparison of biogenic methane emissions from unmanaged estuaries, lakes, oceans, rivers and wetlands, Atmos. Environ., 59, 328-337, 10.1016/j.atmosenv.2012.05.031, 2012.

Osudar, R., Matoušů, A., Alawi, M., Wagner, D., and Bussmann, I.: Environmental factors affecting methane distribution and bacterial methane oxidation in the German Bight (North Sea), Estuar. Coast. Shelf Sci., 160, 10-21, doi:10.1016/j.ecss.2015.03.028, 2015.

Osudar, R., Liebner, S., Alawi, M., Yang, S., Bussmann, I., and Wagner, D.: Methane turnover and methanotrophic communities in arctic aquatic ecosystems of the Lena Delta, Northeast Siberia, FEMS Microbiol Ecol, doi: 10.1093/femsec/fiw116, 2016.

Osudar, R., Klings, K., Wagner, D., and Bussmann, I.: Effect of salinity on microbial methane oxidation in freshwater and marine environments, Aquat. Microb. Ecol., accepted.

Overduin, P. P., Liebner, S., Knoblauch, C., Gunther, F., Wetterich, S., Schirrmeister, L., Hubberten, H. W., and Grigoriev, M. N.: Methane oxidation following submarine permafrost degradation: Measurements from a central Laptev Sea shelf borehole, Journal of Geophysical Research-Biogeosciences, 120, 965-978, doi:10.1002/2014jg002862, 2015.

Rachold, V., Bolshiyanov, D. Y., Grigoriev, M. N., Hubberten, H. W., Junker, R., Kunitsky, V. V., Merker, F., Overduin, P. P., and Schneider, W.: Near-shore Arctic Subsea Permafrost in Transition, EOS: Transactions of the American Geophysical Union, 88, 149-156, 2007.

Sapart, C. J., Shakhova, N., Semiletov, I., Jansen, J., Szidat, S., Kosmach, D., Dudarev, O., van der Veen, C., Egger, M., Sergienko, V., Salyuk, A., Tumskoy, V., Tison, J.-L., and Röckmann, T.: The origin of methane in the East Siberian Arctic Shelf unraveled with triple isotope analysis, Biogeosci., 14, 2283-2292, 10.5194/bg-14-2283-2017, 2017, 2017.

Schaal, P.: Diversity of methanotrophic bacteria in the Elbe Estuary, Master thesis, Hochschule Bremerhaven, Bremerhaven, 2016.

Schmale, O., Leifer, I., Deimling, J. S. V., Stolle, C., Krause, S., Kießlich, K., Frahm, A., and Treude, T.: Bubble Transport Mechanism: Indications for a gas bubble-mediated inoculation of benthic methanotrophs into the water column, Cont. Shelf Res., 103, 70-78, doi:10.1016/j.csr.2015.04.022, 2015.

Shakhova, N., and Semiletov, I.: Methane release and coastal environment in the East Siberian Arctic shelf, J. Mar. Syst., 66, 227-243, 2007.

Shakhova, N., Semiletov, I., Leifer, I., Salyuk, A., Rekant, P., and Kosmach, D.: Geochemical and geophysical evidence of methane release over the East Siberian Arctic Shelf, J. Geophys. Res.: Oceans, 115, C08007, doi:10.1029/2009jc005602, 2010.

Shakhova, N., Semiletov, I., Leifer, I., Sergienko, V., Salyuk, A., Kosmach, D., Chernykh, D., Stubbs, C., Nicolsky, D., Tumskoy, V., and Gustafsson, O.: Ebullition and storm-induced methane release from the East Siberian Arctic Shelf, Nature Geosci, 7, 64-70, 2014.

Silvennoinen, H., Liikanen, A., Rintala, J., and Martikainen, P.: Greenhouse gas fluxes from the eutrophic Temmesjoki River and its Estuary in the Liminganlahti Bay (the Baltic Sea), Biogeochem., 90, 193-208, doi:10.1007/s10533-008-9244-1, 2008.

Stanley, E. H., Casson, N. J., Christel, S. T., Crawford, J. T., Loken, L. C., and Oliver, S. K.: The ecology of methane in streams and rivers: patterns, controls,and global significance, Ecol. Monogr., 86, 146-171, 2016.

Steinle, L., Graves, C. A., Treude, T., Ferre, B., Biastoch, A., Bussmann, I., Berndt, C., Krastel, S., James, R. H., Behrens, E., Boning, C. W., Greinert, J., Sapart, C.-J., Scheinert, M., Sommer, S., Lehmann, M. F., and Niemann, H.: Water column methanotrophy controlled by a rapid oceanographic switch, Nature Geosci., 8, 378–382, doi:10.1038/ngeo2420, 2015.

Striegl, R. G., Dornblaser, M. M., McDonald, C. P., Rover, J. R., and Stets, E. G.: Carbon dioxide and methane emissions from the Yukon River system, Glob. Biogeochem. Cycl., 26, doi:10.1029/2012GB004306, 2012.

Taipale, S. J., and Sonninen, E.: The influence of preservation method and time on the delta C-13 value of dissolved inorganic carbon in water samples, Rapid Communications in Mass Spectrometry, 23, 2507-2510, 10.1002/rcm.4072, 2009.

Tang, K. W., McGinnis, D. F., Frindte, K., Brüchert, V., and Grossart, H. P.: Paradox reconsidered: Methane oversaturation in well-oxygenated lake waters, Limnol. Oceanogr., 59, 275-284, 10.4319/lo.2014.59.1.0275, 2014.

Tavormina, P. L., Ussler, W., III, and Orphan, V. J.: Planktonic and sediment-associated aerobic methanotrophs in two seep systems along the North American margin, Appl. Environ. Microbiol., 74, 3985-3995, doi:10.1128/aem.00069-08, 2008.

Tavormina, P. L., Ussler, W., Joye, S. B., Harrison, B. K., and Orphan, V. J.: Distributions of putative aerobic methanotrophs in diverse pelagic marine environments, ISME J, 4, 700-710, 2010.

Thornton, B. F., Geibel, M. C., Crill, P. M., Humborg, C., and Mörth, C.-M.: Methane fluxes from the sea to the atmosphere across the Siberian shelf seas, Geophys. Res. Lett., 43, doi:10.1002/2016GL068977, 2016.

Tokoro, T., Watanabe, A., Kayanne, H., Nadaoka, K., Tamura, H., Nozaki, K., Kato, K., and Negishi, A.: Measurement of air-water CO2 transfer at four coastal sites using a chamber method, J. Mar. Syst., 66, 140-149, doi:10.1016/j.jmarsys.2006.04.010, 2007.

Upstill-Goddard, R. C., and Barnes, J.: Methane emissions from UK estuaries: Re-evaluating the estuarine source of tropospheric methane from Europe, Mar. Chem., 180, 14-23, 10.1016/j.marchem.2016.01.010, 2016.

Wahlström, I., and Meier, H. E. M.: A model sensitivity study for the sea–air exchange of methane in the Laptev Sea, Arctic Ocean, Tellus B, 66, 24174, doi.org/10.3402/tellusb.v66.24174, 2014.

Wanninkhof, R., Asher, W. E., Ho, D. T., Sweeney, C. S., and McGillis, W. R.: Advances in quantifying air-sea gas exchange and environmental forcing, Annual Review of Marine Science, 1, 213-244, doi:10.1146/annurev.marine.010908.163742, 2009.

Wanninkhof, R.: Relationship between wind speed and gas exchange over the ocean revisited, Limnol. Oceanogr.: Methods, 12, 351-362, doi:10.4319/lom.2014.12.351, 2014.

Wen, X., Yang, S., Horn, F., Winkel, M., Wagner, D., and Liebner, S.: Global biogeographic analysis of methanogenic archaea identifies community-shaping environmental factors of natural environments, Frontiers in Microbiology, 8, 10.3389/fmicb.2017.01339, 2017.

Westbrook, G. K., Thatcher, K. E., Rohling, E. J., Piotrowski, A. M., Pälike, H., Osborne, A. H., Nisbet, E. G., Minshull, T. A., Lanoiselle, M., James, R. H., Hühnerbach, V., Green, D., Fisher, R. E., Crocker, A. J., Chabert, A., Bolton, C., Beszczynska-Möller, A., Berndt, C., and Aquilina, A.: Escape of methane gas from the seabed along the West Spitsbergen continental margin, Geophys. Res. Lett., 36, L15608, doi:10.1029/2009GL039191, 2009.

Wiesenburg, D. A., and Guinasso, N. L.: Equilibrium solubilities of methane, carbon monoxide and hydrogen in water and sea water, J. Chem. Eng. Data, 24, 356-360, 1979.

Table 1. The median values of important parameters (methane concentration and oxidation rate, fractional turnover rate k', turnover time, relative abundance and diversity of methanotrophs) in the different water masses. A one-way analysis of variance (ANOVA) was performed to test for significant differences of the log-transformed data between the water masses.

	Median for "Riverine water"	Median for "Mixed water"	Median for "Polar water"	DF / p[1]
CH_4 [nmol L^{-1}]	22	19	26	**94 / 0.03 ***
MOX [nmol L^{-1} d^{-1}]	0.419	0.089	0.400	68 / 0.18
k' [d]	0.011	0.006	0.028	**68 / < 0.001 *** **
Turnover time (d)	91	167	36	
%MOB	0.81	0.19	0.03	**23 / <0.001 *** **
"estimated diversity" [OTUs / station] [2]	4	3	2	**23 / 0.01 ** **

1 results of the ANOVA with degrees of freedom (DF) and level of significance (p).

2 operational taxonomic unit (OTU)

Table 2. Linear correlation between the methane concentration versus different environmental parameters split into three water masses with their whole respective data set. Analysis was performed with log transformed data; the r^2-values, the level of significance (p) and the positive or negative correlation (+/-) are shown. Bold numbers indicate a significant correlation ($p<0.05$).

	"Riverine water" (n = 13)	"Mixed water" (n = 22)	"Polar water" (n = 24)
Temperature	**(+) 0.38 / 0.02**	(+) 0.003 / 0.74	(-) 0.10 / 0.04
Salinity	(-) 0.23 / 0.13	(+) 0.03 / 0.25	(-) 0.0001 / 0.93
O_2	**(-) 0.73 / <0.001**	(-) 0.02 / 0.36	(-) 0.006 / 0.65
DOC[1]	(+) 0.002 / 0.89	(+) 0.01 / 0.31	(-) 0.0003 / 0.94
TDN[2]	(-) 0.0006 / 0.95	**(+) 0.27 / 0.01**	(+) 0.11 / 0.12
Sediment CH_4	n.d.	n.d.	**(+) 0.33 / < 0.001**

n.d. not determined due to insufficient number of data points

1 dissolved organic carbon (DOC)

2 total dissolved nitrogen (TDN)

Table 3. Linear correlation between the methane oxidation rate (MOX) and the fractional turnover rate (k') versus different environmental parameters split into three water masses with their whole respective data set. Analysis was performed with log transformed data; the r^2-values, the level of significance (p), and the positive or negative correlation (+/-) are shown. Bold numbers indicate a significant correlation ($p<0.05$).

	"Riverine water" (n = 6)		"Mixed water" (n = 9)		"Polar water" (n = 11)	
	MOX	k'	MOX	k'	MOX	k'
Temperature	**(+) 0.77 / 0.02**	**(+) 0.84 / 0.01**	(+) 0.01 / 0.77	(+) 0.004 / 0.87	(-) 0.02 / 0.69	(-) 0.07 / 0.41
Salinity	(-) 0.30 / 0.26	(-) 0.43 / 0.16	(+) 0.30 / 0.12	**(+) 0.46 / 0.04**	(+) 0.05 / 0.52	(+) 0.17 / 0.21
O_2	(-) 0.33 / 0.23	(-) 0.30 / 0.26	(-) 0.006 / 0.83	(-) 0.07 / 0.48	(-) 0.03 / 0.67	(-) 0.001 / 0.92
DOC[1]	(+) 0.29 / 0.27	(+) 0.46 / 0.14	(-) 0.009 / 0.80	(+) 0.02 / 0.75	(+) 0.004 / 0.85	(+) 0.007 / 0.80
TDN[2]	(-) 0.02 / 0.80	(-) 0.002 / 0.93	(+) 0.30 / 0.13	(+) 0.27 / 0.08	(+) 0.31 / 0.08	(+) 0.12 / 0.16
Methane	**(+) 0.98 / <0.001**	**(+) 0.96 / <0.001**	**(+) 0.80 / < 0.001**	**(+) 0.73 / <0.001**	**(+) 0.56 / 0.01**	(+) 0.13 / 0.31

1 dissolved organic carbon (DOC)

2 total dissolved nitrogen (TDN)

Table 4. The occurrence and association of the MISA OTUs to different water masses, their assignation to known methanotrophic groups and the results of a Kruskal Wallis test for significant differences in occurrence (*, $p < 0.05$).

MISA OTU	Assignation	Riverine	Mixed	Polar	Kruskal Wallis	Association
OTU-557		3	3	**9**	0.06	Polar
OTU-535	Group Z **	**6**	**6**	3	**0.02 ***	River /mixed
OTU-485	*Methylococcus capsulatus* ***	3	2	2	0.4	
OTU-460		**3**	**3**	0	0.06	River /mixed
OTU-445	OPU-1 **	4	3	4	0.5	
OTU-398		**1**	0	0	0.2	River
OTU-362		**4**	**5**	2	0.1	River /mixed
Median number of OTUs / sample		6	5	4	**0.02***	

** assignation according to (Tavormina et al., 2010)

*** assignation according to (Schaal, 2016)

Table 5. Comparison of diffusive methane flux from the water column into the atmosphere of this region and temperate and polar shelf seas (in μmol m^2 d^{-1}).

Authors	Area	Range	Median
Calculated from dissolved methane concentrations (bottom-up)			
This study	Lena Delta (2 coastal stations of Transect 4)	4–163	24 536
(Bussmann, 2013a)	Buor-Khaya Bay	2 -85	34
(Shakhova and Semiletov, 2007)	Northern parts of Buor-Khaya Bay	4–8	
(Wahlström and Meier, 2014)	Modelled flux for Laptev Sea	6 ± 1	
(Mau et al., 2015)	North Sea with stratified water column in summer	2 -35	9
(Mau et al., 2015)	North Sea in winter, including methane seepage	52–544	104
(Borges et al., 2016)	Southern North Sea, summer 2010, near shore	426 ± 231	
(Steinle et al., 2017)	Eckernförde Bay, Baltic Sea	6–15	8
(Myhre et al., 2016)	West off Svalbard with CH_4 seepage.	Up to 69	3
(Mau et al., 2017)	Coastal waters of Svalbard	-17–173	2
(Graves et al., 2015)	Coastal waters of Svalbard	4–20	
(Fenwick et al., 2017)	North American Arctic Ocean	-0.4–4.9	1.3
Calculated, modelled from atmospheric data (top-down)			
(Thornton et al., 2016)	ice free Laptev Sea		94
(Myhre et al., 2016)	West off Svalbard with CH_4 seepage	207–328	
(Shakhova et al., 2014)	Ebullitive flux around Lena Delta	6250 - 39375	

880

Fig. 1

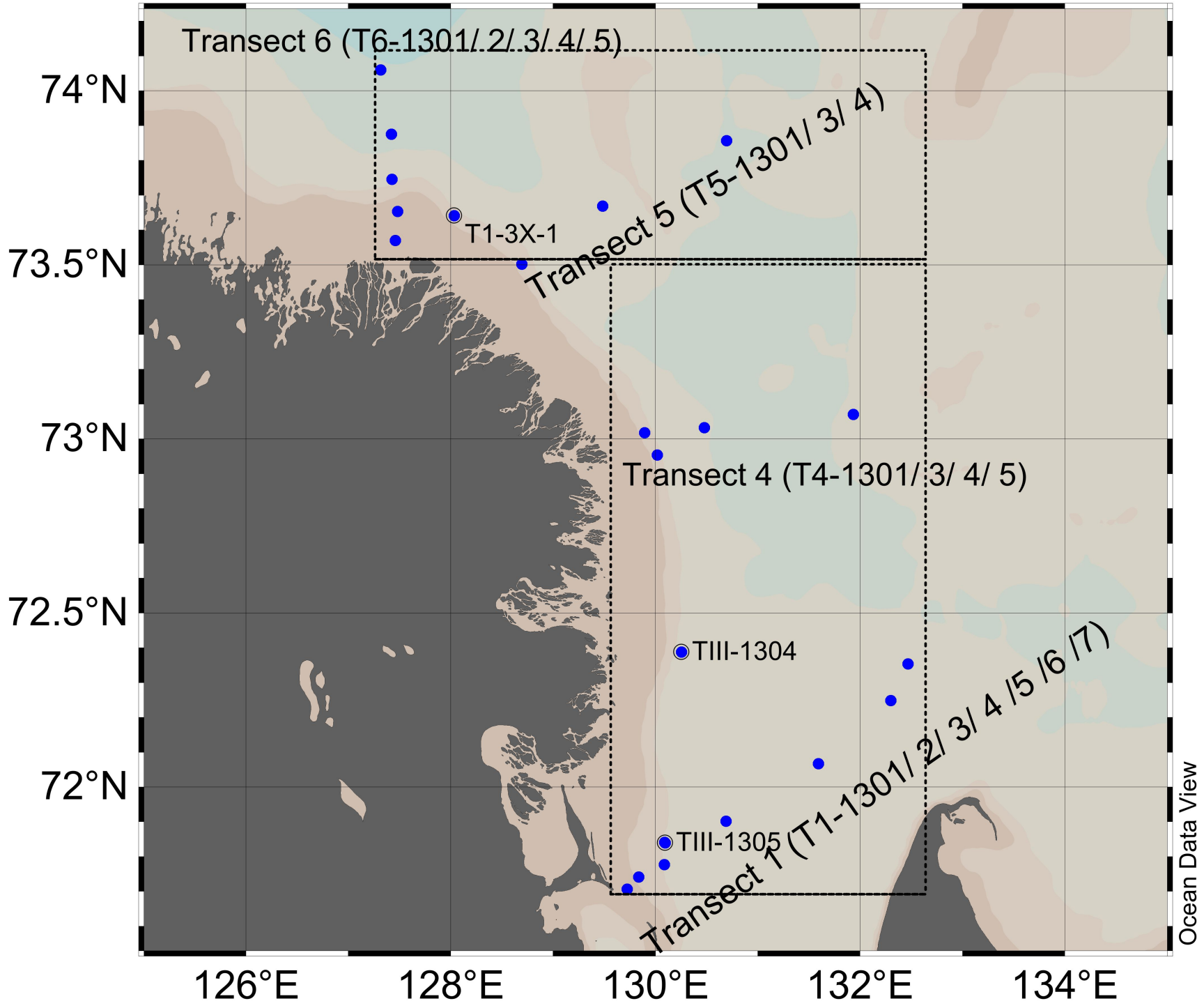
Transect 6 (T6-1301/ 2/ 3/ 4/ 5)
Transect 5 (T5-1301/ 3/ 4)
T1-3X-1
Transect 4 (T4-1301/ 3/ 4/ 5)
TIII-1304
TIII-1305
Transect 1 (T1-1301/ 2/ 3/ 4 /5 /6 /7)
74°N
73.5°N
73°N
72.5°N
72°N
126°E
128°E
130°E
132°E
134°E
Ocean Data View

Fig. 2 A

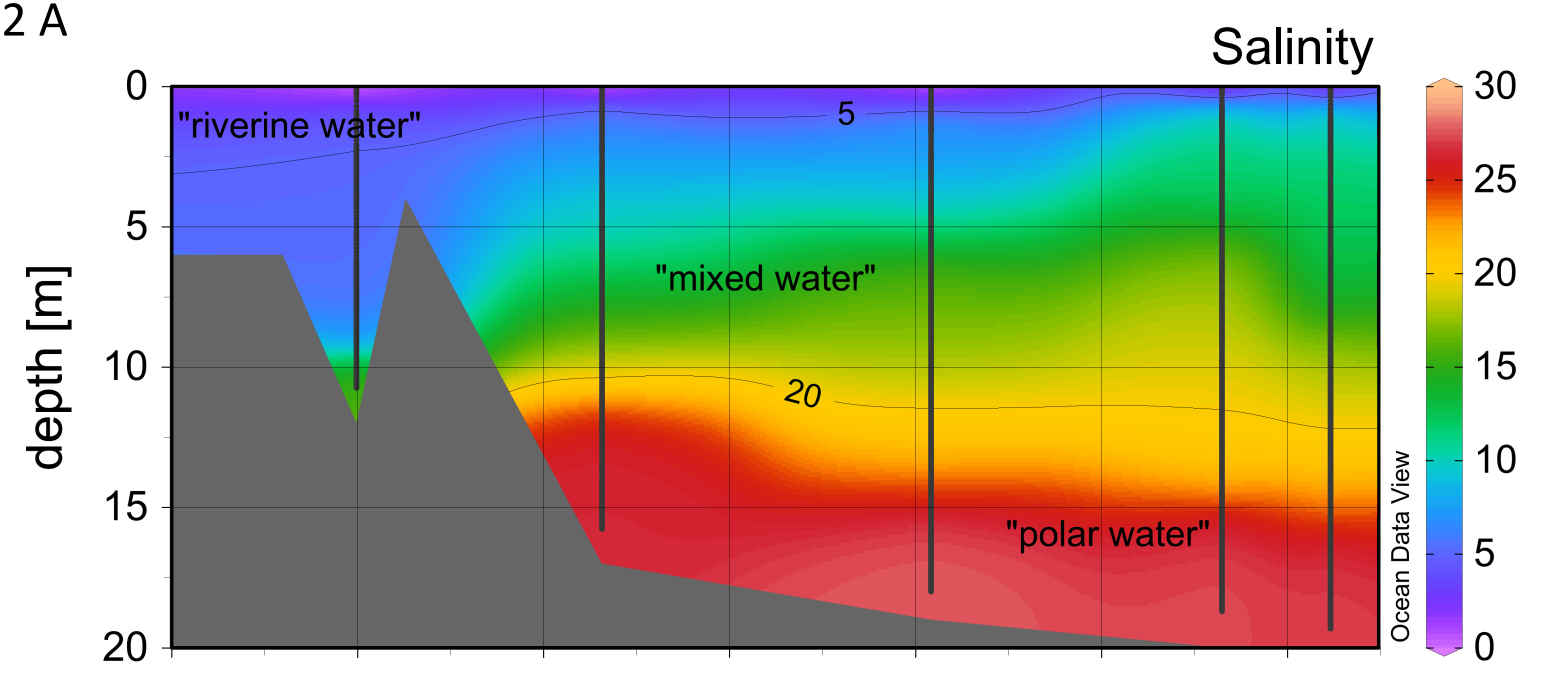
Salinity
"riverine water"
"mixed water"
"polar water"
5
20
depth [m]
0
5
10
15
20
Ocean Data View
30
25
20
15
10
5
0

Fig. 2 B

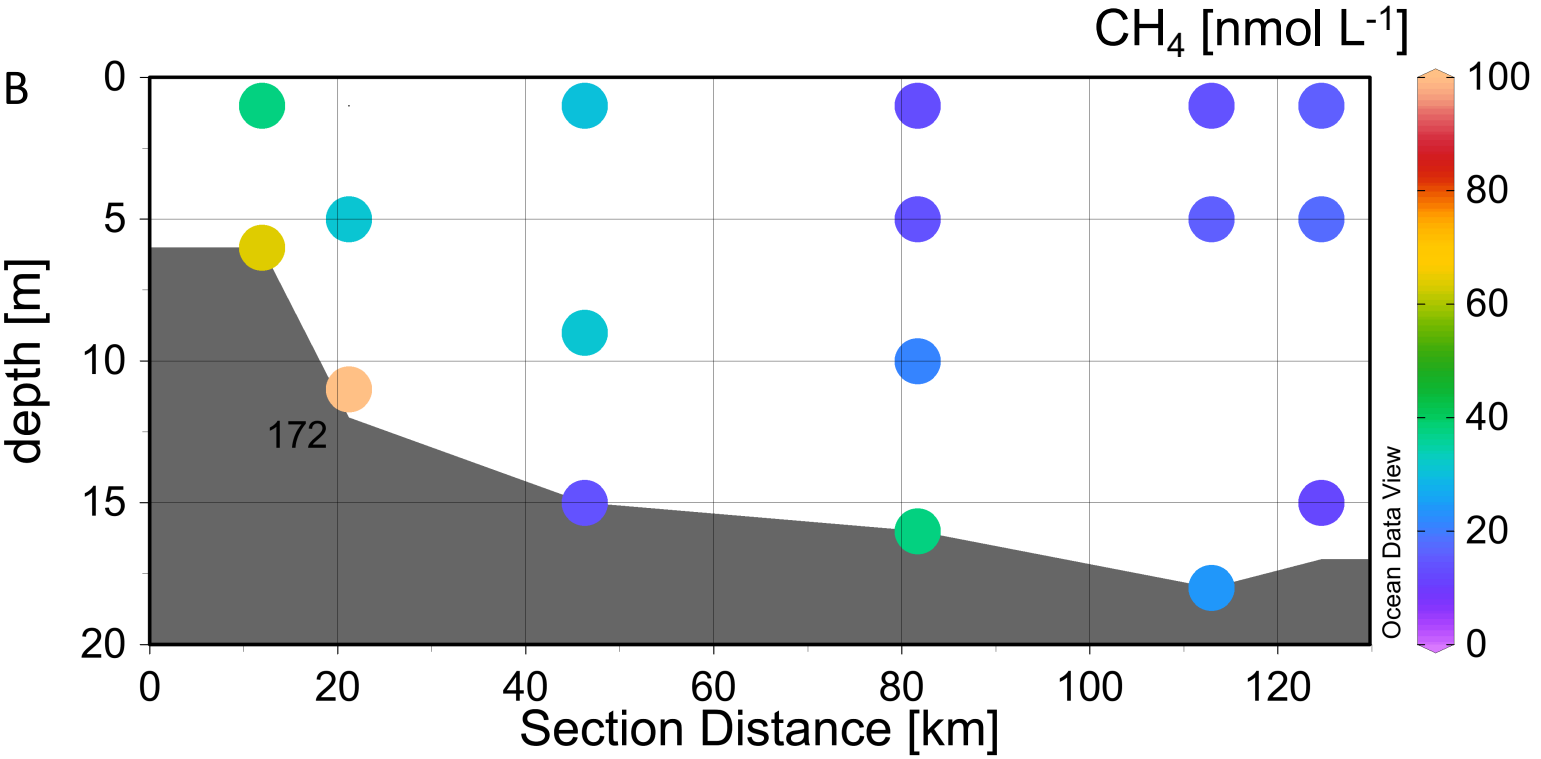
CH4 [nmol L-1]
172
depth [m]
0
5
10
15
20
0
20
40
60
80
100
120
Section Distance [km]
Ocean Data View
100
80
60
40
20
0

Fig. 3

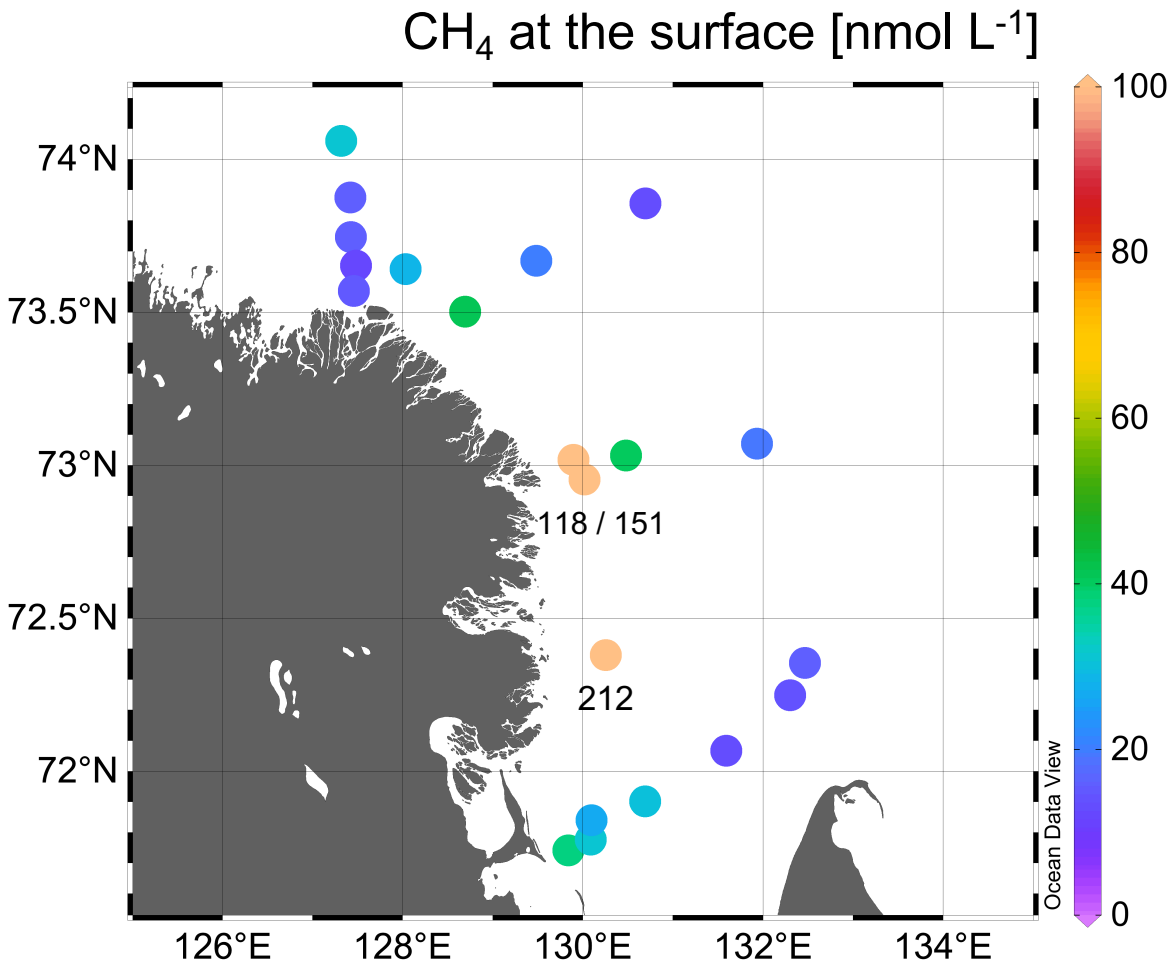
CH4 at the surface [nmol L-1]
74°N
73.5°N
73°N
72.5°N
72°N
126°E
128°E
130°E
132°E
134°E
118 / 151
212
100
80
60
40
20
0
Ocean Data View

Fig. 4

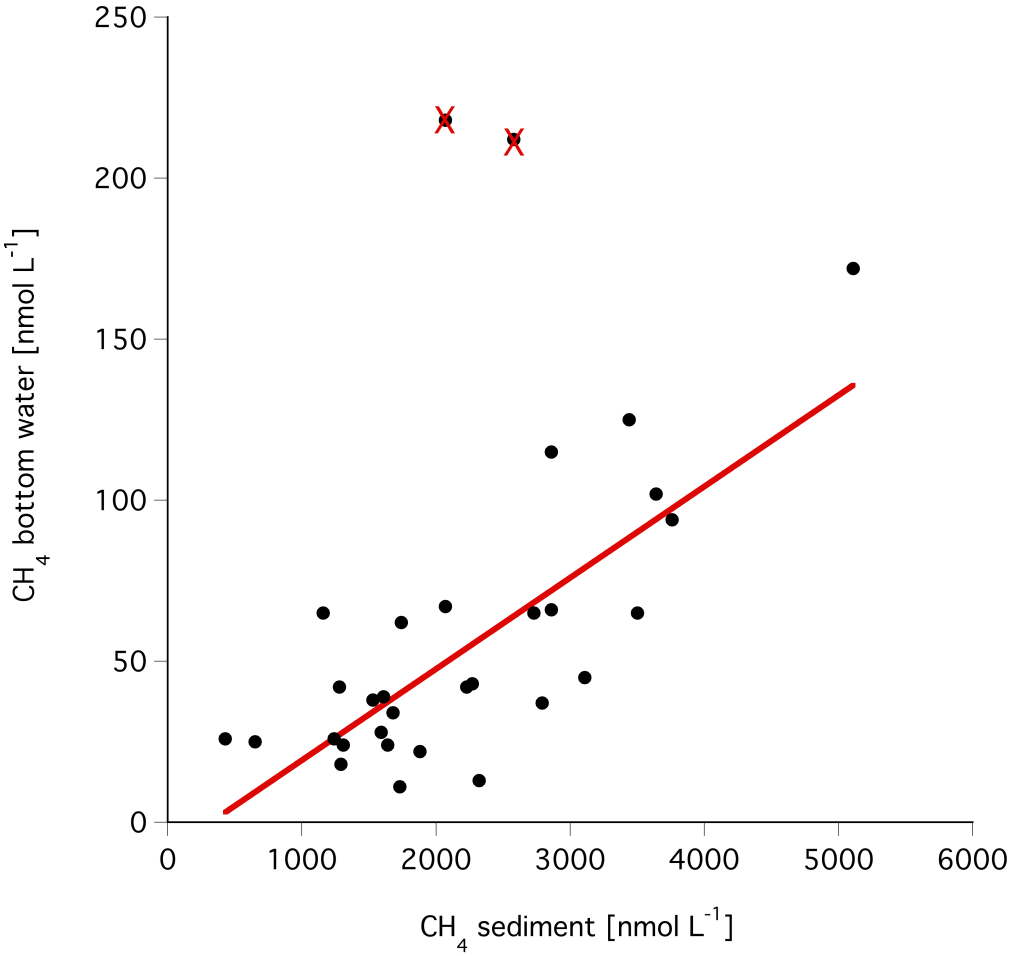
250
200
150
100
50
0
0
1000
2000
3000
4000
5000
6000
CH4 bottom water [nmol L-1]
CH4 sediment [nmol L-1]

Fig. 5

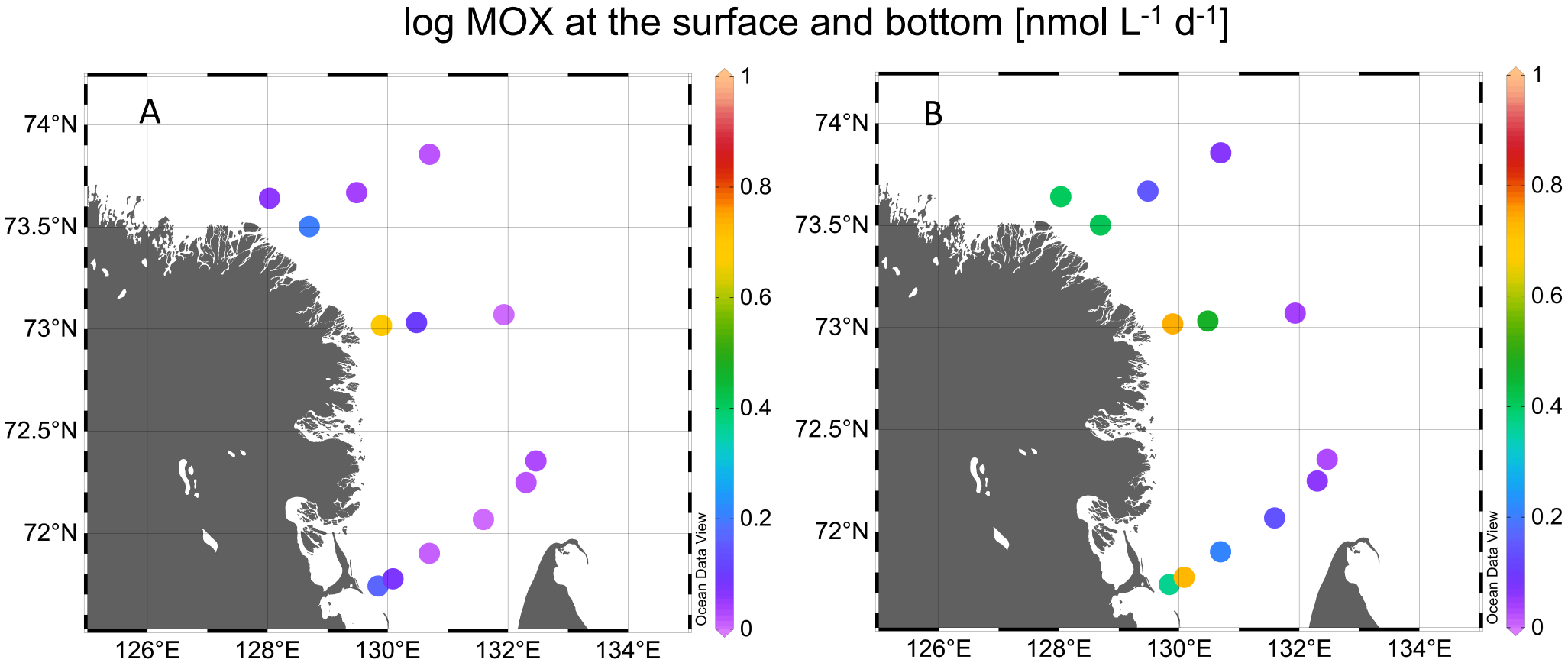
log MOX at the surface and bottom [nmol L-1 d-1]
A
B
74°N
73.5°N
73°N
72.5°N
72°N
126°E
128°E
130°E
132°E
134°E
1
0.8
0.6
0.4
0.2
0
Ocean Data View

Fig. 6

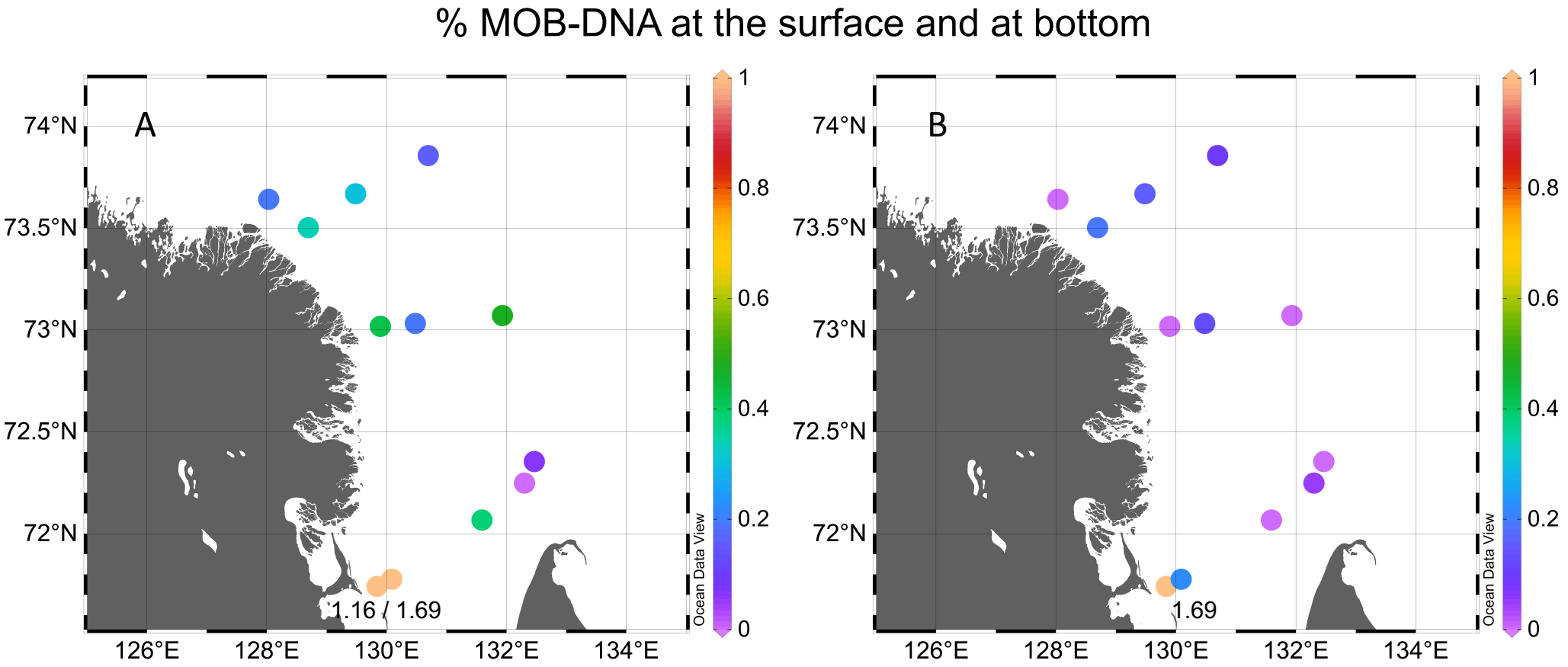
% MOB-DNA at the surface and at bottom
A
B
74°N
73.5°N
73°N
72.5°N
72°N
126°E
128°E
130°E
132°E
134°E
1.16 / 1.69
1.69
1
0.8
0.6
0.4
0.2
0
Ocean Data View

Fig. 7

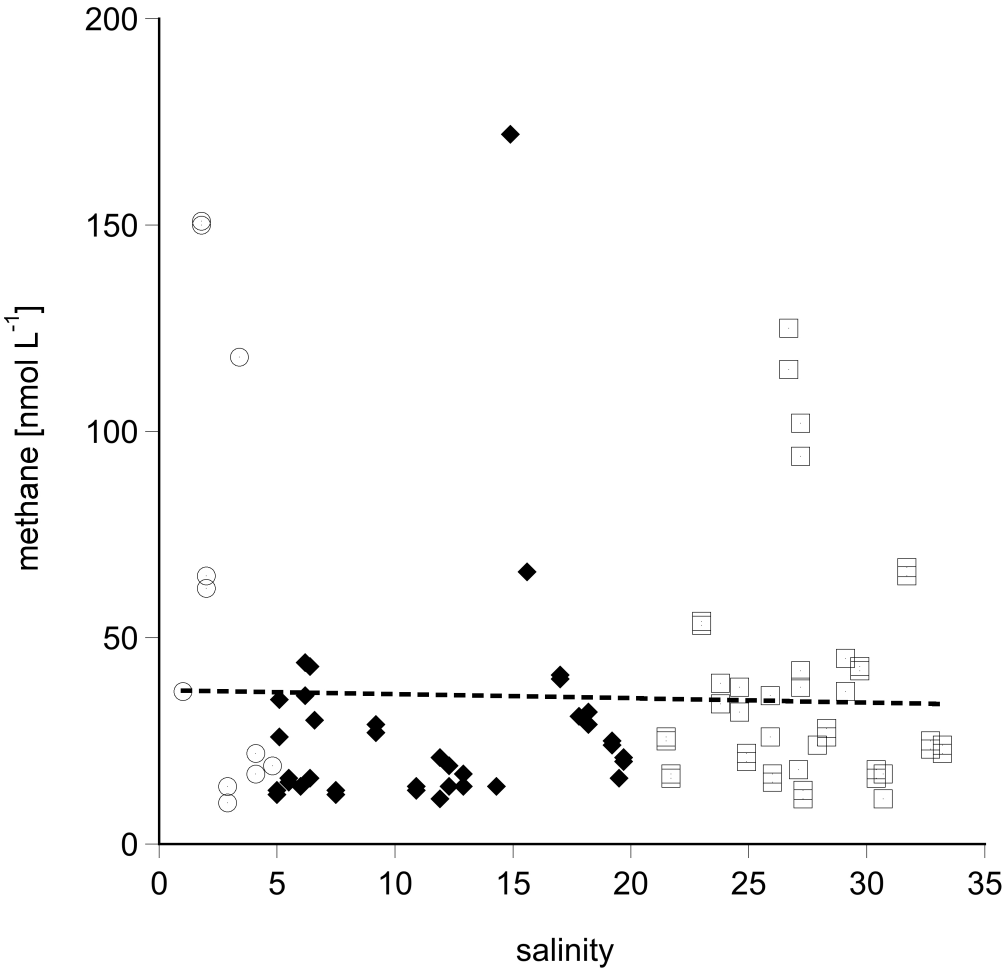

Fig. S1

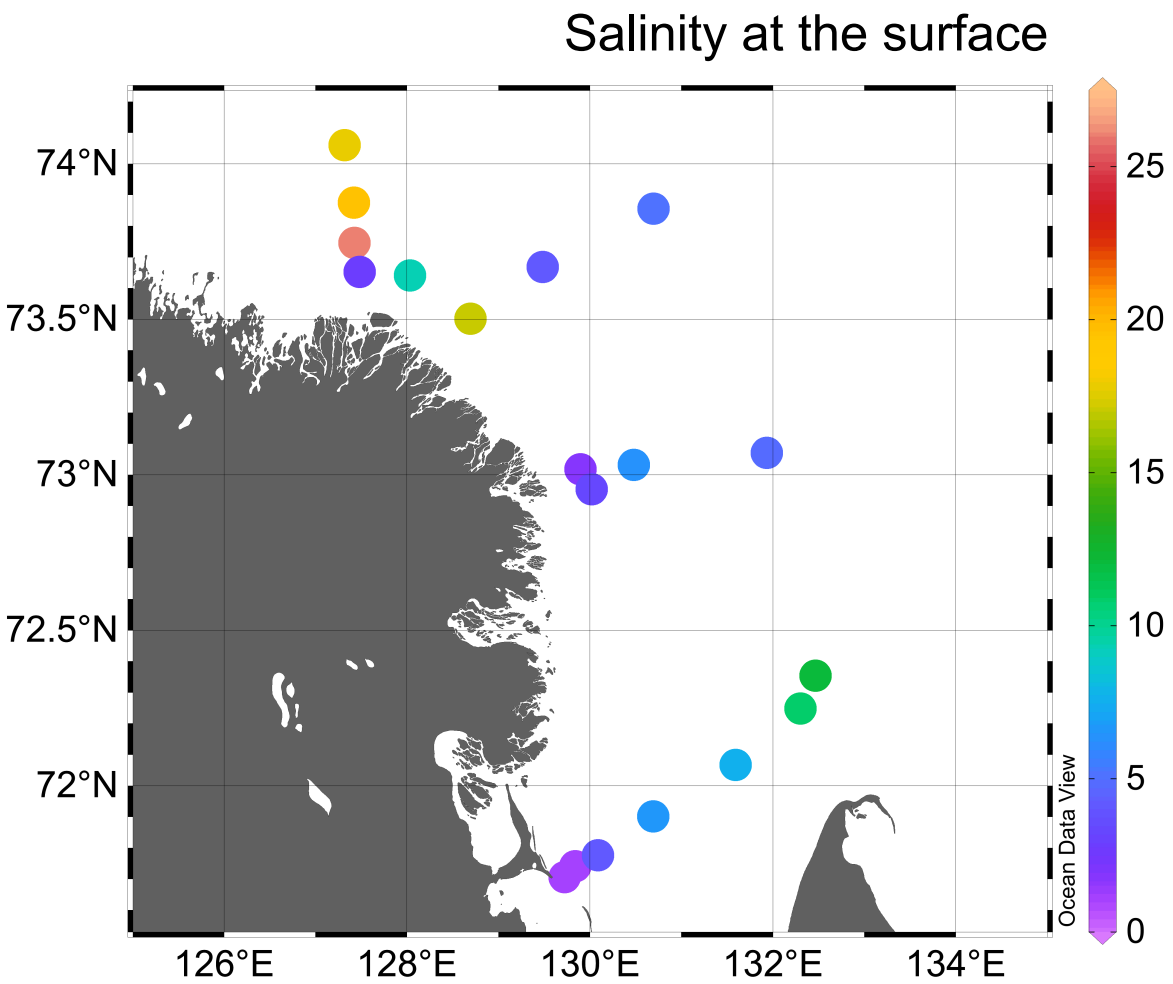
Salinity at the surface
74°N
73.5°N
73°N
72.5°N
72°N
126°E
128°E
130°E
132°E
134°E
25
20
15
10
5
0
Ocean Data View